



# MONASH University

## **The Effect of Grouping in Human Crowd Movement**

Viet Vo

A thesis submitted for the degree of *Master of Philosophy* at

Monash University in October 2016

Faculty of Information Technology

## **Copyright notice**

© Viet Vo, 2016.

Except as provided in the Copyright Act 1968, this thesis may not be reproduced in any form without the written permission of the author.

## Abstract

Human crowd modelling has gained importance for floor plan designs and crowd movement management. It increases the need for more realistic modelling of human-like behaviours (Helbing, 2005). The state of the art in modelling studies often focuses on homogeneous crowds. Grouping behaviour has been rarely addressed. Social studies show that crowds are often inhomogeneous, which are containing different social groups. How groups in crowds interact with each other has been rarely investigated. Exploring the interactions of groups in such inhomogeneous crowds becomes important to understand its impact on crowd movement. Therefore, this study aims to model the dynamics of inhomogeneous crowds including group interactions.

This study starts by building a model that captures the grouping behaviour of individuals in an inhomogeneous crowd. The formation of grouping and non-grouping behaviours was investigated by simulating the model in a narrowing corridor, a turning corridor, a T-intersection corridor, and a corridor with an obstacle. The results of the simulations of grouping and non-grouping behaviours were analysed to explore which behaviour was effective for crowd movement.

This study found that grouping behaviour helped to achieve potential flow rates by preventing turbulence. In contrast, non-grouping behaviour created turbulent flows of individuals and inefficient movement. This study suggests that letting groups stay together is potentially effective for crowd management when a large number of individuals are egressing the venue.

## Declaration

This thesis contains no material which has been accepted for the award of any other degree or diploma at any university or equivalent institution and that, to the best of my knowledge and belief, this thesis contains no material previously published or written by another person, except where due reference is made in the text of the thesis.

Signature:



Print Name: Viet Vo

Date: October 31, 2016

## Acknowledgements

I would like to thank all the people who made this thesis possible.

First of all, my deepest gratitude goes to my supervisors, Prof. Bernd Meyer and Dr. Aldeida Aleti. Not only did they support me for technical aspects, but they also encouraged and advised me to gain more research skills in general. I appreciate their hardship, tireless effort to help me during my apprenticeship.

I would also like to thank my lab-mates, for technical discussions, support, reviewing, and for all the fun we've had over the years. They always keep asking me questions, and holding my balance for social and technical life.

Moreover, I offer my thanks to Faculty of IT for financial supporting during my last two months for thesis completion.

Lastly, I declare that I have received editorial assistance in the preparation of this thesis from Julie Holden in the form of guidance on English grammar and writing skills. Not only did Holden advise me thesis structure, but also she encouraged me to become a better writer.

# Table of Contents

<b>Abstract .....</b>	<b>iii</b>
<b>1 Introduction.....</b>	<b>1</b>
<b>2 Background Study .....</b>	<b>5</b>
2.1. Context of Real-world Crowd Behaviours .....	5
2.1.1. Individual, following, and rioting behaviours.....	6
2.1.2. Grouping behaviour .....	7
2.2. Basic Human Crowd Modelling Approaches.....	9
2.2.1. Agent-based Modelling Approach .....	9
2.2.2. Cellular Automata Modelling Approach .....	11
2.2.3. Force-based Modelling Approach.....	11
2.2.3.1. Reynold “Boids” Model.....	12
2.2.3.2. A Vicsek Model.....	14
2.2.3.3. A Social Force Model.....	15
2.3. State of The Art in Modelling Human Crowd Behaviours .....	17
2.3.1. Agent Modelling Approach for Representing Following Behaviour.....	17
2.3.2. A Cellular Automata Modelling Approach for Representing Following Behaviour.....	18
2.3.3. A Force-based Approach for Representing Following Behaviour .....	19
<b>3 Research Questions and Methodology .....</b>	<b>21</b>
3.1. Research Questions .....	21
3.2. Research Methodology.....	21
<b>4 Modelling the Grouping Behaviour of Individuals in a Homogeneous Crowd.....</b>	<b>25</b>
<b>5 Modelling the Existence of Groups in An Inhomogeneous Crowd.....</b>	<b>31</b>
5.1. Modelling the Interaction between In-group Members and Out-of-group Members .....	31
5.2. Modelling Autonomous Movement of Individuals in a Crowd.....	34
<b>6 The Emergence of Clusters in Crowd Movement.....</b>	<b>36</b>
6.1. Simulations of Grouping and Non-grouping Behaviours.....	36
6.2. Floor Plans and Metrics for Investigating Grouping and Non-grouping Behaviours.....	39
6.3. Results of the Difference between Grouping and Non-grouping Behaviours.....	41
6.3.1. The Difference in Narrowing Corridor.....	42
6.3.2. The Difference in Turning Corridor.....	48
6.3.3. The Difference in T-intersection Corridor.....	53
6.3.4. The Difference in Corridor with an Obstacle .....	58
6.4. Analysis of the Difference between Grouping and Non-grouping Behaviours .....	63
<b>7 Conclusion and Future Work .....</b>	<b>65</b>
7.1. Conclusion .....	65
7.2. Future Work .....	65
<b>References .....</b>	<b>66</b>

# List of Figures

<b>Figure 1.</b> Obstacle design for crossing corridors .....	2
<b>Figure 2.</b> Crowd's following behaviour in a smoke-filled room caused by fire.....	6
<b>Figure 3.</b> Northern Ireland fans during Sunday's UEFA Euro 2016 Qualifier against Finland.....	8
<b>Figure 4.</b> Above view at Boston Marathon bombings on April 15, 2013 (CNN, 2013).....	9
<b>Figure 5.</b> The flow chart of agent-based modelling approach (Macal and North, 2011) .....	10
<b>Figure 6.</b> The conceptual idea of the original CA model (Daniel, 2012).....	11
<b>Figure 7.</b> Steering behaviours in “boids” model.....	12
<b>Figure 8.</b> Social Force Model.....	15
<b>Figure 9.</b> Lane formation and turbulence phenomena .....	17
<b>Figure 10.</b> The integration of CA-based and agent-based modelling approaches .....	19
<b>Figure 11.</b> A two- individual system in one dimensional space .....	26
<b>Figure 12.</b> The distance between two individuals through parameter settings of base model.....	26
<b>Figure 13.</b> The comfortable distances $\delta$ of a homogeneous crowd at different combinations ( $R$ , $A$ ).....	29
<b>Figure 14.</b> The formation of two groups in an inhomogeneous crowd when setting.....	33
$A=20$ , $R = 40$ , $c = 1.0$ .....	33
<b>Figure 15.</b> The formation of groups formed clusters.....	33
<b>Figure 16.</b> Purity measurement at different parameter combinations of ( $A$ , $R$ , $c$ ) .....	34
<b>Figure 17.</b> Social forces acting on individual $p$ .....	34
<b>Figure 18.</b> Grouping behaviour in a long corridor .....	36
<b>Figure 19.</b> Non-grouping behaviour in a long corridor .....	37
<b>Figure 20.</b> Narrowing corridor .....	40
<b>Figure 21.</b> Turning corridor .....	40
<b>Figure 22.</b> T-intersection .....	40
<b>Figure 23.</b> Corridor with obstacle.....	40
<b>Figure 24.</b> Observation of grouping and non-grouping behaviours in a narrowing corridor.....	42
<b>Figure 25.</b> Flowrate distributions in the narrowing corridor .....	43
<b>Figure 26.</b> The heat map of the flowrate percentage difference in the narrowing corridor.....	44
<b>Figure 27.</b> A testing distribution in the narrowing corridor.....	45
<b>Figure 28.</b> The turning angle distribution of grouping and non-grouping behaviours in the narrowing corridor .....	45
<b>Figure 29.</b> The heat map showing the KL distances in the narrowing corridor when setting $c=1.4$ .....	46
<b>Figure 30.</b> The heat map showing the KL distances in the narrowing corridor when setting $c=1.6$ .....	46
<b>Figure 31.</b> The heat map showing the KL distances in the narrowing corridor when setting $c=1.8$ .....	46
<b>Figure 32.</b> The heat map showing the KL distances in the narrowing corridor when setting $c=2.0$ .....	47
<b>Figure 33.</b> The influence networks of two behaviours in the narrowing corridor with setting.....	47
$A=24.0$ , $R = 34.0$ , and $c = 1.4$ .....	47
<b>Figure 34.</b> The observation of grouping and non-grouping behaviours in a turning corridor.....	49
<b>Figure 35.</b> Flowrate distributions of two behaviours in the turning corridor.....	49
<b>Figure 36.</b> The heat map of the flowrate percentage difference in the turning corridor .....	50
<b>Figure 37.</b> The testing distribution in the turning corridor.....	50
<b>Figure 38.</b> The heat map showing the KL distances in the turning corridor with setting $c=1.4$ .....	51

<b>Figure 39.</b> The heat map showing the KL distances in the turning corridor with setting $c=1.6$ .....	51
<b>Figure 40.</b> The heat map showing the KL distances in the turning corridor with setting $c=1.8$ .....	51
<b>Figure 41.</b> The heat map showing the KL distances in the turning corridor with setting $c=2.0$ .....	52
<b>Figure 42.</b> The influence networks of two behaviours in the turning corridor with setting.....	52
$A=20.0$ , $R=36.0$ , $c = 1.4$ .....	52
<b>Figure 43.</b> The observation of grouping and non-grouping behaviours in a T-intersection corridor.....	53
<b>Figure 44.</b> The flowrate distributions of two behaviours in the T-intersection corridor .....	54
<b>Figure 45.</b> The heat map of the flowrate percentage difference in the T-intersection .....	55
<b>Figure 46.</b> The testing distribution in the T-intersection corridor.....	55
<b>Figure 47.</b> The heat map showing the KL distances in the T-intersection corridor with setting $c=1.4$ .....	56
<b>Figure 48.</b> The heat map showing the KL distances in the T-intersection corridor with setting $c=1.6$ .....	56
<b>Figure 49.</b> The heat map showing the KL distances in the T-intersection corridor with setting $c=1.8$ .....	56
<b>Figure 50.</b> The heat map showing the KL distances in the T-intersection corridor with setting $c=2.0$ .....	57
<b>Figure 51.</b> The influence networks of two behaviours in the T-intersection corridor with setting .....	57
$A=20.0$ , $R=36.0$ , and $c = 1.4$ .....	57
<b>Figure 52.</b> The observation of grouping and non-grouping behaviours in the corridor with an obstacle .....	58
<b>Figure 53.</b> The flowrate distributions of grouping and non-grouping behaviours in the corridor with obstacle .....	59
<b>Figure 54.</b> The heat map of the flowrate percentage difference in the corridor with an obstacle .....	60
<b>Figure 55.</b> The testing distribution in the corridor with an obstacle .....	60
<b>Figure 56.</b> The heat map of the KL distances in the corridor with obstacle with setting $c=1.4$ .....	61
<b>Figure 57.</b> The heat map of the KL distances in the corridor with obstacle with setting $c=1.6$ .....	61
<b>Figure 58.</b> The heat map of the KL distances in the corridor with obstacle with setting $c=1.8$ .....	61
<b>Figure 59.</b> The heat map of the KL distances in the corridor with obstacle with setting $c=2.0$ .....	62
<b>Figure 60.</b> The influence networks of two scenarios in the corridor with an obstacle .....	62
with setting $A=18.0$ , $R=40.0$ , $c = 1.4$ .....	62
<b>Figure 61.</b> In-group and out-of-group forces acting on a tracked individual caused by grouping behaviour.....	63
<b>Figure 62.</b> In-group and out-of-group forces acting on an tracked individual caused by non-grouping behaviour ...	64





# 1 Introduction

Over 70% of the world's population is predicted to live in cities by 2050 (Weidmann, 2012). Rapid urbanisation and population growth will create inevitable challenges in the effort of planning infrastructure. The increased migration into central cities will affect the number of public events and the increase in the number of participants. Event accidents have been reported as increasing. For example, one of the disasters that occurred at the Station Nightclub, USA (2003) caused nearly one hundred deaths. Investigators of the disaster found that the rate of egress at the main entrance of the building was low because a crowd-crush disrupted the flow through the front exit (Grosshandler, 2005). Therefore with the increase of public events and potential accidents, optimising indoor floor plans and managing crowd movement becomes important to potentially save human lives.

Performing experiments on real-world human crowds to evaluate floor plans and crowd management plans is time consuming and expensive. For instance, a seminal study, which tried to optimize the widths of subway corridors in 1958, recruited more than 200 male students and designed experiments in a school to understand the relationship between speed and passage widths before deploying experiments in a subway (Hankin, 1958). Nowadays, urban designers and event organizers use crowd behaviour simulations instead of performing experiments with real-world human crowds. Crowd behaviour simulations are based on behaviour models that imitate human-like behaviours. Researchers observe real-world crowds at various places and extract individual's behaviours to produce human-like behaviours of virtual pedestrians in crowd simulations. Using crowd behaviour simulations aims to reduce time consuming and costs than deploying experiments on real-world crowds. Moreover, simulation also allows urban designers and event organisers to evaluate various floor plans before starting to construct them. Typical floor plans, which have been used widely, are narrowing corridors, turning corridors, T-intersection of merging flows, and corridors with obstacles inside (Helbing, 2002; Moussaid, 2011).

Crowd modelling, the process of building behaviour models to explore how crowd behaviours emerge from individuals' interactions, becomes an important research area for crowd simulation. Previous studies have investigated and modelled a number of real-world crowd behaviours. These behaviours include individual behaviour, and following behaviour (Helbing, 2000; Pelechano, 2006). Virtual pedestrians perform these behaviours and avoid collision while they are moving to reach an exit door in a floor plan. Well-established models, which aim to present these behaviours, are agent-based (Wijermans, 2013), cellular automata (Vizzari, 2013), and force-based models (Helbing, 1995). By using these behaviour models, crowds that are moving and containing these

behaviours are simulated to investigate the capacity of proposed infrastructures such as which floor plans are effective. The effectiveness of crowd movement in these floor plans is often measured by flow rate, which is the average number of pedestrians exiting floor plan per second.

For instance, one of the findings from studies simulating individual behaviour found that placing pillars in a narrowing corridor creates a higher flow rate than the flow rate of crowd in the corridor without pillars (Helbing, 2005). Moreover, corridors where counter flows often happen should have separate obstacles, such as barriers, railings, and columns, to improve the flow rate (Helbing, 2005). Figure 1 describes these obstacles in corridors.

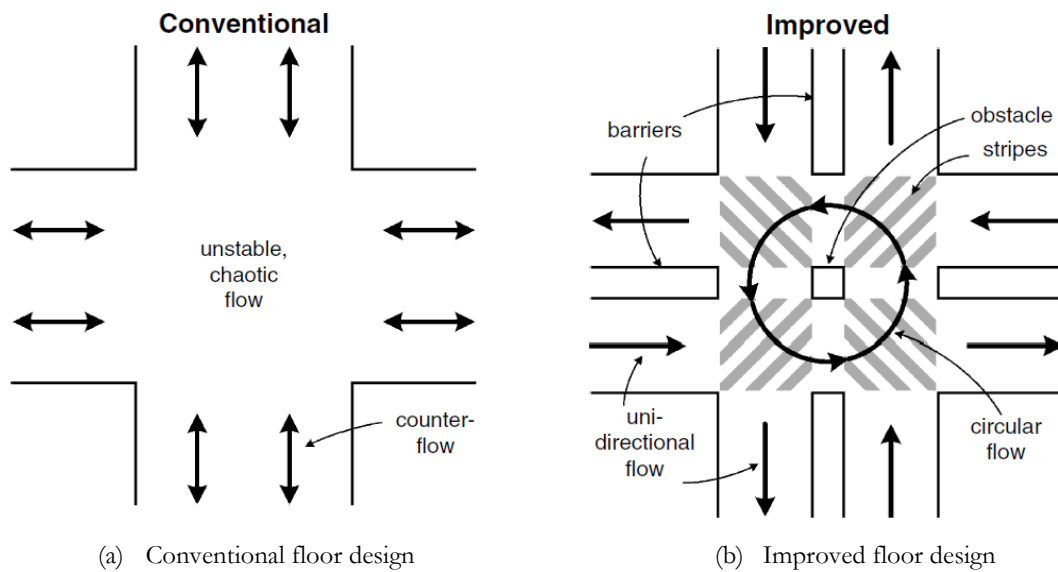


**Figure 1.** Obstacle design for crossing corridors

Figure 1.a presents a conventional design at a crossing area. This design easily creates chaotic and turbulent flow. In contrast, Figure 1.b shows an improved design in which barriers and obstacles are added to improve crowd flows (Helbing, 2005).

Simulating allows the variation of different settings of corridors and obstacles to be tested. Therefore, the author found that obstacles helped to prevent pedestrians from using small space of opposite flow for overtaking behaviour. The study also suggested that having two separate doors for opposite flows would be better than having only one door with double width (Helbing, 2005). Similarly, simulating individual behaviour in crowds has been used for seeking optimal designs for football stadiums. For instance, a study developed evacuation scenarios to optimize a stadium's spectator areas (Liu, 2011). Using simulations helped the study's authors found that the confluence at intersection areas had a significant impact on the flow rate. In general, current studies often relies on designing obstacles to enhance the flow rate.

Real-world crowd simulations are not only used for floor plan designs but also crowd movement management. For instance, a study simulated the evacuation of crowds participating a music festival event on a ship caused by fires (Ronchi, 2016). The study simulated crowds of unconnected individuals and then suggested that evacuation plans should take into account the evacuation time at crossing corridors rather than the final evacuation time at main entrances. Due to the fact that intersection areas could makes the space clogged and crowd turbulent.

Therefore, simulating human-like behaviours is important for floor plan designs and crowd movement management at densely populated places. It allows urban designers to test various designs before implementing and event-organisers to examine different crowd movement plans without deploying experiments with real-world crowds.

Current studies have mostly investigated the individual behaviour of crowd members (Helbing, 2002; Hoogendoorn, 2012). However, in busy public places where individuals do not walk alone, real-world crowds often contain more than one social group (Reicher, 2011; Stott, 2007). A crowd in large areas like shopping malls and football stadiums typically consists of individuals that belong to different communities such as families or different football teams. In this study, the term “group” is used to describe individuals who have similar characteristics and tend to stay together while moving. In contrast, the term “cluster” refers to a spatial structure of a crowd. These clusters may or may not merge together in a crowd. The interaction of different groups in a crowd leads to the formation of clusters. The term “inhomogeneous” is used to describe a crowd that contain different groups.

For instance, given a crowd of fans supporting two different football teams at a stadium, fans of each team have to interact with people who are the same and different team-supporters. Individuals in a crowd prefer to stay close to people who are familiar in order to maximize communication during movement. Consequently, clusters emerge in crowd movement in which each cluster contains people who are the same team-supporters.

Identifying solutions that can save human lives as many as possible when participants are egressing floor plans becomes important. Previous studies often focus on optimising floor plans, and exploring the impact of individual and follow behaviours on crowd movement. However, investigating how groups in crowds interact with each other has rarely been studied, while grouping behaviour often occur in normal conditions and emergency situations. The formation from groups’ interactions becomes important to examine its impact on crowd movement. Therefore, this study aims to explore the effect of grouping behaviour in crowd movement using typical floor plans,

which are narrowing corridors, turning corridors, T-intersection of merging flows, and corridors with obstacles inside. The study is expected to answer whether grouping behaviour can potentially benefit flowrate and prevent turbulence.

The scope of this research is at investigating grouping behaviour of individuals in inhomogeneous crowds in simulation environment. This research is based on a mathematical model that presents the grouping behaviour of individuals in a homogeneous crowd. The model is then extended to present the existence of different groups in inhomogeneous crowds. The simulations of grouping and non-grouping behaviours are constructed by using the extension version of the model.

The flow rates of grouping behaviour are compared to the flow rates of non-grouping behaviour in typical floor plans. Furthermore, the formation of crowds caused by these behaviours is compared to investigate which behaviour is effective for crowd movement. The study contends that grouping behaviour generates higher flow rates by reducing turbulence in the crowd movement.

This thesis is organized to seven chapters. Chapter 2 presents background research of the study. Chapter 3 proposes research questions and methodology respectively. Chapter 4 details the base model of this study. Chapter 5 discusses how to model the existence of groups to form clusters in crowd. Chapter 6 analyses the effect of the emergence of clusters in crowd movement. Chapter 7 summarises the study and presents recommendations for future works.

## 2 Background Study

This chapter draws together related studies that underpin this research. They vary from different research studies including social, physical modelling, and computer simulation studies. The reason why this study investigates different fields is because human crowd modelling is an interdisciplinary research area that often relies on social observations to describe human behaviours and then mathematically formulates them in simulation environments based on basic physical modelling approaches.

Social studies collect evidence of real-world crowd behaviours and explore them by using social factors (Reicher and Drury, 2011), while physical studies propose fundamental approaches that are often based on the modelling of other living organisms, such as flocks of birds, and particle systems (Reynolds, 1987; Vicsek, 1995; Helbing, 1995). Typical tasks that computer scientists often focus on include the construction of simulation models of human-like behaviours and the investigation of these models when testing with different floor layout plans (Helbing, 2000; Helbing, 2005; Moussaïd, 2010; Sun, 2014). Thus, this research investigates these related studies in order to propose research questions in next chapters.

Section 2.1 presents the context of typical crowd behaviours that have been found by social studies. Section 2.2 details fundamental modelling approaches from physical studies. Section 2.3 presents the state of the art of well-known studies that aim to model crowd behaviours in simulation environments.

### 2.1. Context of Real-world Crowd Behaviours

Investigating how actual pedestrians in crowds interact with each other is necessary for modellers to simulate virtual pedestrians. Modellers often pay more attention to behaviours that occur commonly in reality. Therefore, social studies aim to collect evidences, to seek and to explain which behaviours arise in both normal and emergency situations. Behaviours that are often found in crowd movement are individual, following, rioting, and grouping behaviours (Challenger, Clegg, Robinson, 2010). While individual, following, and rioting behaviours typically occur in emergency situations, grouping behaviour is often found in both normal conditions and emergency situations. This subsection presents brief context of these behaviours and for which situations they apply. It aims to explain how current modelling studies formulate these behaviours in simulation environment.

### 2.1.1. Individual, following, and rioting behaviours

Uncontrollable behaviours typically occur in emergency situations such as panic evacuations and riotous events, rather than normal situations. Crowd members in such crowds often feel nervous and physical dangers potentially occur within crowds (Helbing, 2007; 2012).

Individual behaviour is used to describe individuals who behave more individualistically in crowds and neglect social norms in evacuation situations (Quarantelli, 1954, 1957). Interactions between individuals become more physical (Helbing, 2000). When escape movement routes are limited and physical interactions increase, individuals feel trapped and start to push, trample, and crush each other (Janis and Leventhal, 1968; Killan, 1972).

Following behaviour is a term used to describe emergency situations where individuals are nervous and they lack independence. Consequently, they follow other people in the assumption that they can help them escape faster (Almeida, 2011). This behaviour is visualised in Figure 2.

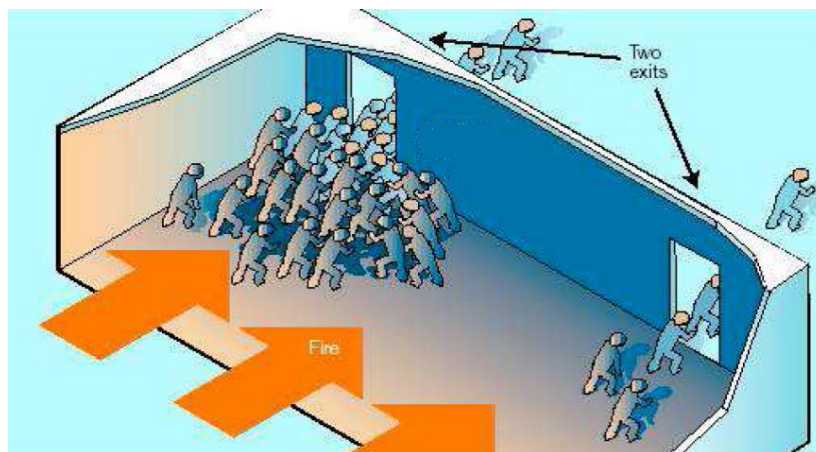


**Figure 2.** Crowd's following behaviour in a smoke-filled room caused by fire

In riotous events, several behaviours including avoidance and rioting are exhibited. These behaviours are often carried out by antisocial individuals with a mass of followers. Real-world crowds in such events comprise rioters, civilians and police in which each individual has different actions. Rioters and followers raise the violent attention by throwing fires, smashing cars while police try to dominate rioter's area, to reduce a crowded atmosphere, and to protect civilians (Myers, 2004; Torrens, 2013). Participants in riotous events often have geographic behaviours of spatial cognition, locomotion, steering and spatial strategy (Davies, 2013).

Individual, following, and rioting behaviours are often used to describe how individuals behave in emergency situations rather than in normal conditions. These behaviours often become the main focus for modellers when simulating evacuation scenarios. However, modelling behaviours that

occur in normal conditions at densely populated places is also necessary. It allows to create optimal urban infrastructure and to plan crowd management scenarios in public events. Therefore, there is a need for investigating behaviours that occur more frequently in both normal and emergency situations, such as grouping behaviour.

### **2.1.2. Grouping behaviour**

While individual, following, and rioting behaviours often occur in emergency situations, grouping behaviour arises more commonly in normal conditions and emergency situations.

A physical crowd often contains more than one social group (Drury, 2004; Cocking, 2008, 2009). A group is a social unit comprising members who stand in relationships with other members in the same group. Grouping behaviour can be easily seen in normal situations. A social study highlighted that the majority, 74%, of crowds at the intersection areas of main roads in UK were with one or more friends (Aveni, 1977). People belong to groups because of social ties. Members in a group often are family members, colleagues, school mates, or people who have the same characteristics or interests. Members of the same group feel more familiar to stay together than staying in different groups. Staying together with familiar members helps them to maximize communication, to reduce stress levels and depression, and to increase optimism in emergency situations (Haslam, 2005; Dougall, 2001). Clusters emerge spatially in crowds because of the existence of these social groups. These clusters occur as spatial coherence when people share their social identities in crowds (Drury, Cocking, and Reicher, 2009). A cluster in a crowd has a number of individuals who are of the same group.

At dense places, such as stadiums and shopping malls, the majority of the public is comprised of different groups. A social experiment interviewed participants at an American stadium and found that there was only a quarter of the crowd population attending as individual (Aveni, 1977). Other social studies have given the same findings (Stott, 2007). For instance, a large crowd in sporting events often contains opposing groups that support different sport teams in these events. Supporters in each group move collectively against other opposing groups to maintain social coherence. Consequently, clusters emerge spatially in the crowd. Figure 3 shows a crowd containing fans of two opposing groups at a stadium. The two groups form clusters in which each cluster contains fans of the same team.





**Figure 3.** Northern Ireland fans during Sunday's UEFA Euro 2016 Qualifier against Finland

Two fan groups are supporting Northern Ireland and Finland football teams. Clusters emerge spatially in the crowd. Clusters are highlighted in this figure.

Furthermore, grouping behaviour was often seen in previous emergency situations of football stadium fires, football stampede disasters, car-bomb and train accidents (Drury, Cocking and Reicher, 2009). Evacuees of these situations often felt fearful and shared their social identities to each other. Commonly social identities are family roles, and the different types of rescuers such as police and fight fighters. Evacuees often stuck to their rescuers when sharing social identities (Challenger, Clegg, Robinson, 2010). Strangers even grouped together although they were unfamiliar with each other before. Consequently, clusters emerge spatially in such crowds. For instance, grouping behaviour was seen during the London bombing of July, 2005 when individual commuters helped each other and united into clusters (Drury, 2009). Another evidence of grouping behaviour was seen in Boston Marathon bombings caused by terrorist attack on April 15, 2013 (Dugan, 2015; Price, 2015). Figure 4 was captured by Aaron Tang through a window of his office (CNN, 2013). During this evacuation, each cluster in a crowd contained either members of a family, or collection of people incorporating and helping each other.



**Figure 4.** Above view at Boston Marathon bombings on April 15, 2013 (CNN, 2013)

Clusters emerge spatially in the crowd. They are highlighted in this figure.

While individual, rioting, and following behaviours typically occur in emergency situations, social studies have provided sufficient evidence for the existence of grouping behaviour in both normal conditions and emergency situations. Due to the existence of social groups in crowds, clusters emerges spatially during crowd movement.

Simulating these behaviours is important to explore their impacts on crowd movement, which is useful for designing floor plans and planning crowd movement for safety purposes (Helbing, 2005). The simulation typically acquires mathematical models that make virtual individuals perform these behaviours in different simulation environments. Therefore, the next section aims to present fundamental modelling approaches, which are primarily inspired by biological and physical studies.

## **2.2. Basic Human Crowd Modelling Approaches**

Modern simulation studies often rely on or are improved from basic modelling approaches that were proposed in biological and physical studies. Typically basic modelling approaches, which have been applied most in modern studies, are agent-based, cellular automata, and force-based models (Hoogendoorn, 2013). This section details these fundamental approaches.

### **2.2.1. Agent-based Modelling Approach**

The agent-based modelling approaches aim to model autonomous and interacting agents (Georgeff, 1989). The approach pays attention to the decision making process of agents. Autonomous agents have their own attributes and could be comparable to a real person in the simulation environment. Agents react to certain situations and adapt to a dynamic environment.

Agent's behaviours are regulated by a set of decision rules. In general, designing autonomous agents contains two parts:

- Reflect how agents interact with the virtual world and make different decisions based on perception.
- Describe the agents' own attributes and abilities so that the crowd simulation is heterogonous.

This model allows to create various agents and to simulate the communicability between agents. The following diagram conceptualises the flow chart of an agent-based modelling approach (Macal and North, 2011; Winter, 2012).

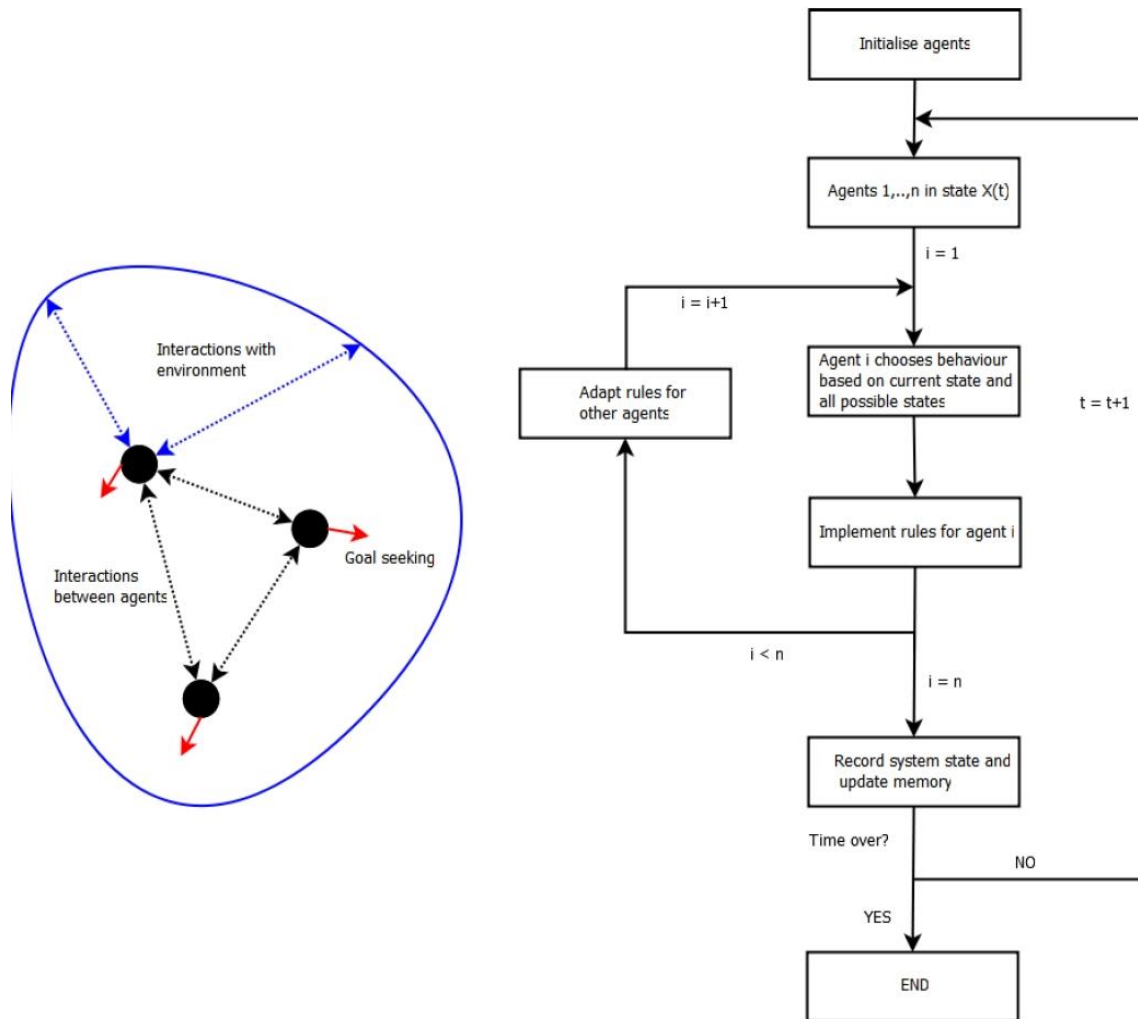


**Figure 5.** The flow chart of agent-based modelling approach (Macal and North, 2011)

During their lifetime, agents interact with the environment and other agents while performing desired actions. The heterogeneity between agents makes them have different reactions to environment and neighbours, or movement route choice based on their predefined attributes (Pelechano, 2006). Crowd's behaviour emerges when agents interact with their local neighbours. An agent-based modelling approach is considered as a natural way to describe crowds and it is flexible to define agents (Bonabeau, 2002). However, this approach does not propose a consistent

mechanism for defining behaviours rules and agent's attributes. Therefore, current studies using this approach often have different rules and attributes to define agents. (Bonabeau, 2002).

### 2.2.2. Cellular Automata Modelling Approach

In contrast to agent-based approaches, cellular automata (CA) based approaches describe space as a uniform grid with attributes to each cell. Attributes are updated based on the rules that in the relation to neighbourhood of the cell. Movement can only be simulated by cells' attributes. For instance, moving between cells changes the attribute of the cells to be occupied or unoccupied. The CA model was originally proposed by J. Von Neumann to generalise biological systems and it has been used in different applications for nearly fifty years (Neumann, 1966). Figure 6 generalises the idea of the model.

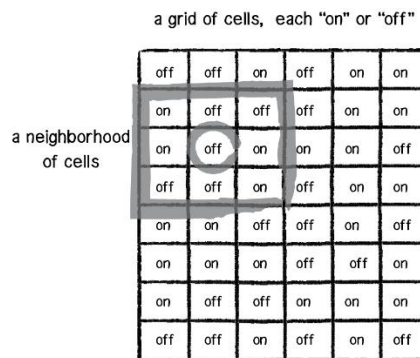


**Figure 6.** The conceptual idea of the original CA model (Daniel, 2012)

Figure 6 shows the idea of CA model in which cells are in different states "on" and "off" to present whether the cells are occupied. CA-based approaches often customise the original CA model by contributing more states of each cell and creating field layers of the grid. These solutions aim to make the model more flexible for modelling different applications (Hafstein, 2004).

### 2.2.3. Force-based Modelling Approach

In contrast to agent-based and cellular automata modelling approaches, a force-based approach is applied more widely to simulate the interactions of individuals in living organisms. It does not focus on creating behaviour rules or dividing space into grids. The force-based approach represents the motion of individuals in crowds in continuously spatial and temporal space from interacting forces. The interactions between individuals in a crowd, and the interactions between individuals and environment are considered as social force elements that influence the movement of



individuals. For instance, given an individual  $p$ , its velocity  $\vec{v}_p$  at time  $t$  is defined by a Langevin equation:

$$\frac{d\vec{v}_p}{dt} = f(X, t) \quad (1)$$

where  $F(X, t)$  integrates possible forces acting on individual  $p$  at time  $t$ . Possible forces are various, such as:

- The interaction force caused by other individuals in the crowd
- The obstacle force that caused by obstacles. This force allows individual  $p$  to avoid the obstacles

Force-based approaches are various for modelling the movement of individuals in different living organisms, such as flocks of birds or particles, and human crowds. The earliest model in this approach simulated the motion of bird flocks, which was named as “Boids” (Reynolds, 1986). The later model simulated the interaction between particles in huge flocks (Vicsek, 1995). Another model was then designed specifically to simulate human crowd (Helbing, 1995, 2000). This section reviews these three models because they are the most typical models that have been used commonly by current simulation studies following this approach.

### 2.2.3.1. Reynold “Boids” Model

The “Boids” model is the earliest biologically inspired model that simulates flocks based on the combination of a finite number of behaviours. The model proposes three simple steering behaviours to describe how birds fly together based on their interactions (Reynolds, 1986). Figure 7 presents these three types of steering behaviours. They are separation, cohesion, and alignment. These behaviours create corresponding force directions acting on each bird.

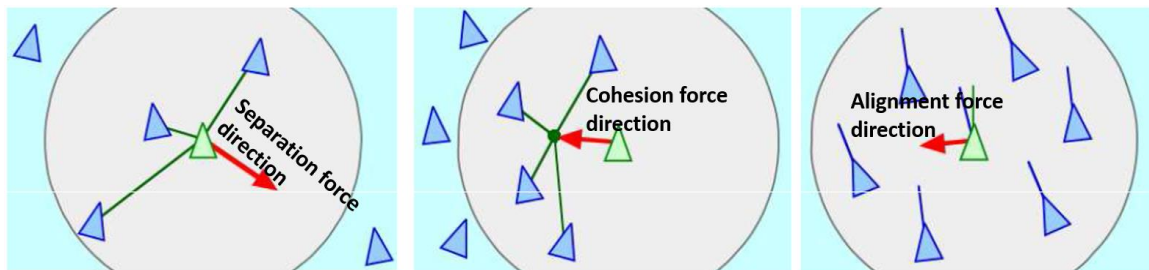


**Figure 7.** Steering behaviours in “boids” model

Separation allows birds steer to avoid collision while cohesion makes birds move toward the average position of other birds. Alignment allows birds move in the direction averaged by other

birds' heading directions. This model combines the directions of steering behaviours and then by added them together to create the force that cause acceleration for each bird. Table 1 presents the parameters of the model and Equations 2-4 present the model.

**Table 1** – “Boids” model's parameters

Parameter	Type
$m$	Scalar value to present mass of bird
$\vec{x}$	Position vector to present position of bird $i$
$\vec{v}$	Velocity vector to present position of bird $i$
$\vec{d}^{\text{seperation}}$	Vector presents separation to avoid other birds
$\vec{d}^{\text{cohesion}}$	Vector presents cohesion to fly toward other birds
$\vec{d}^{\text{alignment}}$	Vector presents alignment to fly in the direction of other birds
$\vec{d}^{\text{steering}}$	Vector present the motion of direction caused by steering behaviours
$ f $	Scalar value to present the force magnitude that can act on bird
$v_{\text{max}}$	Scalar value to present maximum speed a bird can fly

$$\vec{d}^{\text{steering}} = \vec{d}_i^{\text{seperation}} + \vec{d}_i^{\text{cohesion}} + \vec{d}_i^{\text{alignment}} \quad (2)$$

$$\vec{f}(t) = \text{truncate}(\vec{d}^{\text{steering}}, |f|) \quad (3)$$

$$\vec{a}(t) = \vec{f}(t) / m \quad (4)$$

At each simulation step, the model only provides a force strength  $|f|$  in the steering direction  $\vec{d}^{\text{steering}}$ . This force strength can be adjusted adaptively to simulate which behaviour is more important. The force then produces an acceleration on each bird that has a weight of mass  $m$ . Equations 5-7 present how to update velocity and position for each bird.

$$\vec{v}(t+1) = \vec{v}(t) + \vec{a}(t) \quad (5)$$

$$|\vec{v}(t+1)| = \text{truncate}(v_{\text{max}}, |\vec{v}(t+1)|) \quad (6)$$

$$\vec{x}(t+1) = \vec{x}(t) + \vec{v}(t+1) \quad (7)$$

The acceleration  $\vec{a}(t)$  is added to the old velocity to create a new velocity  $\vec{v}(t+1)$  that is then truncated by maximum speed  $v_{\text{max}}$ . The new position  $\vec{x}(t+1)$  is identified by adding the final velocity to the old position  $\vec{x}(t)$ .

The model contributes a new concept in combining basic behaviours to create the movement of birds based on interaction forces. It also verifies that the collective motion of flocking organisms originates from the interaction of each bird. The model is also simple and well-understood so that

future studies can easily integrate other additional behaviours, such as seek and flee, and obstacle avoidance (Reynold, 1999).

### 2.2.3.2. A Vicsek Model

While “Boids” model focuses on the combination of a finite number of behaviours, Vicsek model is the first physical model that pays more attention on the interaction range of particles in a flock, due to the fact that nearby particles creates stronger interactions than others that are at further positions (Vicsek, 1995). Vicsek and colleagues modelled flocks in a way that a particle aligns its direction of motion with its neighbours in a defined radius range  $R$ . A particle is propelled by a constant speed and the force caused by neighbours within that range plus with a random noise. The model is presented in Equations 8.

$$\vec{v}(t + 1) = v_0 \frac{\langle \vec{v}_j(t) \rangle_R}{|\langle \vec{v}_j(t) \rangle_R|} + \text{perturbation} \quad (8)$$

The main idea of the model is that at each given time step  $t$ , particle  $i$  is controlled by interactions with its local neighbours in a constant radius  $R$  and a perturbation factor. Here  $\langle \vec{v}_j(t) \rangle_R$  denotes the averaging of the velocities of neighbours in radius  $R$ . The expression  $\frac{\langle \vec{v}_j(t) \rangle_R}{|\langle \vec{v}_j(t) \rangle_R|}$  provides a unit vector pointing in the average direction of motion. The particle  $i$  also has an initial velocity  $v_0$ . The velocity  $v_0$  is set the same for all particles in a flock.

Although “Boids” and Vicsek models aim to simulate the motion of individuals in a flock based on interaction force, they still are different from each other.

- “Boids” model considers the motion of each bird is caused by the interaction with all others in a flock, whereas Vicsek model defines a radius range  $R$  for the interaction.
- “Boids” model uses an independent force strength to produce the magnitude of velocity for each bird as presented in Equations 3-5. In contrast, Vicsek model takes into account the initial velocity  $v_0$  and a perturbation factor to produce the velocity for each particle.

In the standard version of Vicsek model, Vicsek derived the perturbation factor by adding a random angle to the angle corresponding to the average motion direction of particle  $i$ 's neighbourhood. The angel  $\vartheta_i$  of average motion direction and random angle  $\Delta_i$  at time  $t$  are represented as in Equations 9-10.

$$\vartheta_i(t) = \arctan\left(\frac{v_{j,x}}{v_{j,y}}\right) \quad (9)$$

$$\vartheta_i(t + 1) = \vartheta_i(t) + \Delta_i(t) \quad (10)$$

where  $v_{j,x}$  and  $v_{j,y}$  are the x and y coordinates of particle  $j^{\text{th}}$ 's velocity in the neighbourhood of particle  $i$ . The perturbation  $\Delta_i(t)$  is a random number taken from uniform distribution in the interval  $[-\eta\pi, \eta\pi]$ . The randomness of perturbation makes particles have different directions of motion.

Finally, Vicsek models contains only two control parameters that are the density  $\rho$  (number of particles in a volume  $R^d$  (d is the dimension)), and the level of perturbation  $\eta$ .

The common measurements of particles' movement are the average momentum of the particles  $\phi \equiv \frac{1}{N} |\sum_j \vec{v}_j|$  and the correlation between particles' velocity directions. The author found that the average momentum decreases when decreasing the density or increasing the level of perturbation (Bhattacharya and Vicsek, 2010).

To summarise, Vicsek model is used to understand the formation of huge flocks of living organisms, such as flocking of birds, or particles, in which the movement of each particle is affected by neighbours in a defined radius. The model is well-understood since it only contains two parameters. Thus, it can be easily applied to investigate the collective motion of particles when varying the model's parameters.

### 2.2.3.3. A Social Force Model

In contrast to the Vicsek Model, a social force model is specifically constructed for modelling human crowds (Helbing, Vicsek, and Molnar, 1995; Helbing, 2000). The social force model presents the change of an individual's motion based on forces caused by exiting target, other pedestrians, and obstacles. Figure 8 illustrates this idea.

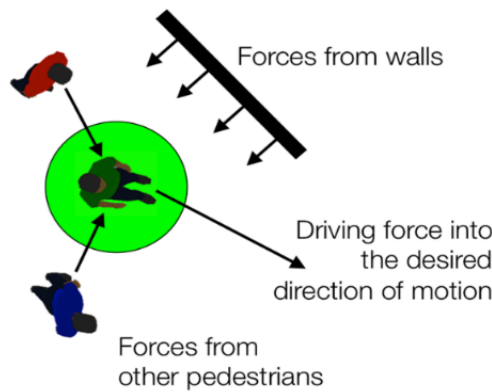


**Figure 8.** Social Force Model



Acceleration of pedestrian  $p$  in crowd is illustrated as follows.

$$\vec{f}_p(t) = \frac{1}{\tau_p} \left( v_p^d(t) \vec{e}_p^d(t) - \vec{v}_p(t) \right) + \sum_{q(\neq p)} \vec{f}_{pq}^{rep}(t) + \sum_{\gamma} \vec{f}_{p\gamma}(t) \quad (11)$$

The model represents that a pedestrian  $p$  at time  $t$  is trying to move with a certain desired speed  $v_p^d(t)$  in a desired direction  $\vec{e}_p^d(t)$  pointing from pedestrian  $p$ 's current position to his target position. Therefore, pedestrian  $p$  tends to correspondingly adapt actual velocity  $\vec{v}_p(t)$  with a certain acceleration time  $\tau_p$ . The acceleration time  $\tau_p$  represents that pedestrian  $p$  changes its current velocity and return to its desired velocity. Pedestrian  $p$ 's acceleration at time  $t$  is also influenced by repulsive forces coming from surrounding pedestrians and obstacles. They are  $\sum_{q(\neq p)} \vec{f}_{pq}^{rep}(t)$  and  $\sum_{\gamma} \vec{f}_{p\gamma}(t)$ , respectively. Repulsive force  $\vec{f}_{pq}^{rep}$  created by neighbour pedestrian  $q$  is given as follows.

$$\vec{f}_{pq}^{rep}(t) = A_{rep} e^{\left( \frac{(R_p + R_q) - d_{pq}(t)}{B_{rep}} \right)} \vec{u}_{qp} \quad (12)$$

where  $A_{rep}$  and  $B_{rep}$  present the strength of interaction force and how sensitive the repulsive force are based on the distance between pedestrians  $p$  and  $q$ , respectively.  $R_p$  and  $R_q$  parameters represent radii of pedestrians  $p$  and  $q$ , and  $(R_p + R_q) \leq d_{pq}$ . Literally, the higher  $B_{rep}$  value means pedestrian  $p$  is more uncomfortable and wants to move further away from pedestrian  $q$ . The exponent function is used to describe that the repulsive force decrease exponentially if  $d_{pq}$  is high. The repulsive force achieves the highest value when pedestrians  $p$  and  $q$  collide ( $R_p + R_q = d_{pq}$ ). Factor  $\vec{u}_{qp}$  is the unit vector pointing from pedestrian  $q$  to pedestrian  $p$  to illustrate the force direction making pedestrian  $p$  avoid pedestrian  $q$ .

The obstacle force between pedestrian  $p$  and wall  $\gamma$  in Equation 11 is represented by using Equation 13.

$$\vec{f}_{p\gamma}(t) = \frac{U}{R_p} e^{\frac{-d_{p\gamma}(t)}{R_p}} \vec{u}_{\gamma p} \quad (13)$$

where  $U$  is a model parameter to represent the strength of obstacle force, and  $\vec{u}_{\gamma p}$  is the unit vector pointing from wall  $\gamma$  to pedestrian  $p$  to make the agent avoid the wall.

In nature, the movement of human crowd have been seen in different self-organization phenomena, such as lane formation and turbulence. Lane formation emerges at places where two flows of pedestrians moving in opposite directions appear spontaneously. The number of lanes and their width vary according to pedestrians' interaction (Helbing, 2005). A turbulence phenomenon leads to unanticipated irregular motion of pedestrians. It is caused by strong and rapid changes of interaction forces in crowds especially at high density areas (Helbing, 2002). Figure 9 shows these phenomena (Helbing, 2000).

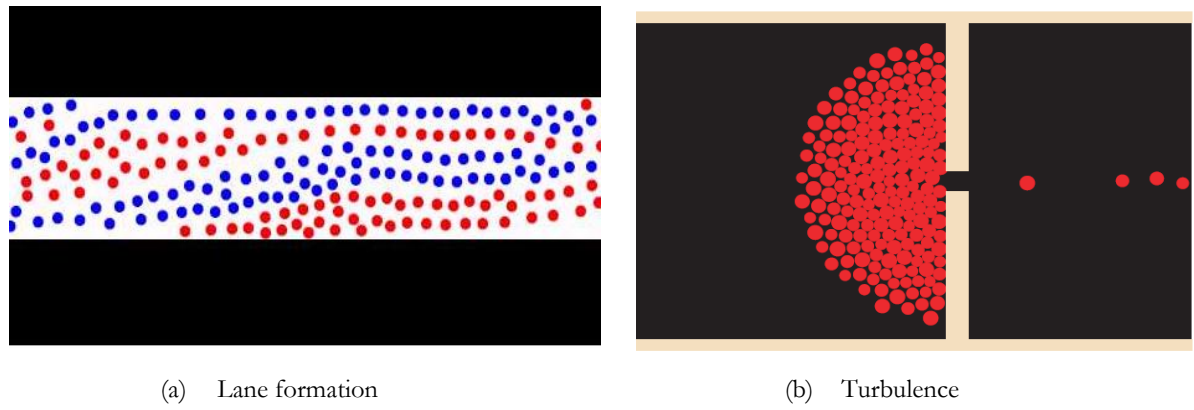


**Figure 9.** Lane formation and turbulence phenomena

The proposed social-force model of Helbing and his colleagues, which is one of the most cited works in crowd modelling, has successfully been used to describe and simulate these self-organization phenomena (Helbing, 2005).

## 2.3. State of The Art in Modelling Human Crowd Behaviours

Social studies have identified typical crowd behaviours that often are seen in reality, such as individual, following, and grouping behaviours. This section examines whether current studies have explored the impact of these behaviours on crowd movement. Only well-known studies from the three fundamental approaches are selected for reviewing in this section.

### 2.3.1. Agent Modelling Approach for Representing Following Behaviour

An agent-based modelling approach allows the creation of inhomogeneous agents and that can be integrated easily with other systems (Weijmen, 2013; Sun, 2014). Generally, there are agent-based studies focusing on the intelligence, reactivity, and communication ability of agents according to their predefined social identity or demographical information.

For instance, each agent can be assigned a specific role, which could be trained as leader or policemen, untrained leader, or follower. Agents follow leaders while they are moving to reach exit gates. Studies using this approach typically investigate the impact of various roles and the number of agents of each role on evacuation duration (Pelecheno, 2006; Shendarkar, 2008). Moreover, behaviour rules are often defined to formulate the interaction between agents, such as they can share route paths that lead to exit gates.

In the trend of more agent-based models being proposed, agent attributes and constraint behaviour rules between those autonomous agents are conducted incrementally to simulate complex scenarios. Current studies in this approach typically focus on the diversity of social roles and behavioural rules to improve the intelligence and reactivity of members (Wijermans, 2013). During the lifetime of agents in simulations, agents' priorities are to move close to predefined leaders.

However, in reality, it is highlighted that evacuees often see the group that they belong to and being different from other group (Drury, Cocking, and Reicher, 2009), agent-based studies rarely investigate the interaction of individuals from different groups. Therefore, investigating the impact of grouping on crowd movement requires exploration.

### 2.3.2. A Cellular Automata Modelling Approach for Representing Following Behaviour

In a cellular automata approach, geometrical layout is divided into cells. By using CA-based approaches, modelling crowd behaviours typically acquires the presence of objects such as obstacles, and exit gates. Obstacles can occupy more than one cell. Every cell in the space can be in different states including free, obstacle, or occupied. Equations 14-16 presents possible states and neighbourhoods of each cell (Vizzari, 2013).

$$\text{Environment} = c_0, c_1, c_2, c_3, \dots \text{ where } \forall c_i: c_i \in \text{Cell} \quad (14)$$

$$\text{neighbours}(c) = \{N(c), S(c), E(c), W(c), NE(c), SE(c), NW(c), SW(c)\} \quad (15)$$

$$\text{State}(c) = s: s \in \{\text{Free}, \text{Obstacle}, \text{Occupied}\} \quad (16)$$

Moreover, every cell has variables of path field, obstacle field, and density field (Suma, 2011). Path field identifies the distance from current cell to destination cell. Obstacle field indicates for every cell the distance from an obstacle or a wall. Density field estimates the crowd density in the surroundings at the current time step  $t$ . Variables at each cell are updated according to a set of local rules or its neighbour cells at each time  $t$ .

There are other studies that integrate CA-based model and agent-based model to simulate agents (Burstedde, 2001). In these studies, an agent has attributes as follows:

- Id: identification number of that agent  $i$
- State: represents agent's current cell that and direction followed in last movement
- Actions: is the set of possible actions when the agent at a specific cell
- Destination: reflects the current path field of the cell where agent  $i$  is in

The relation between a cell's information and individuals within that cell is modelled. This model is sufficient to store sequential states of each cell over the time. Figure 10 presents the integration of agent-based and CA-based approaches to simulate a crowd.

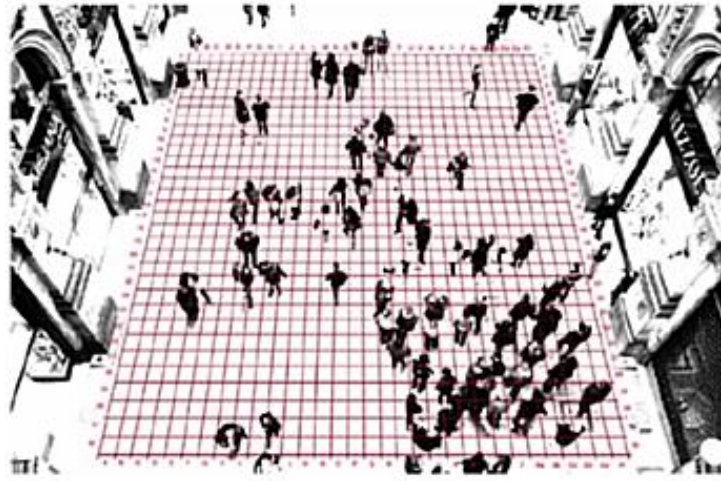


**Figure 10.** The integration of CA-based and agent-based modelling approaches

Following behaviour is represented by estimating the probability of a cell  $c$  that allows agent  $i$  to move towards other members in a crowd (Vihas, 2012; Vizzari, 2013). These studies then often investigate the correlation between crowd population size and crowd average speed in various floor plans. However, studies using CA modelling approach remain the limitations of the original CA model that only allows agents to move into neighbour cells rather than cells at further distances. Therefore, this approach is rarely applied to simulate human crowd self-organization phenomena while the force-based approach is more suitable to produce crowd phenomena (Hoogendoorn, 2013).

### 2.3.3. A Force-based Approach for Representing Following Behaviour

Modelling the following behaviour of members in a small crowd (up to four members) has been proposed by adding a new force element into the social force model (Moussaïd and Helbing, 2010). This force makes members follow the crowd's centre position instead of being attracted by each other. Individual in crowd continuously adjusts its position to reduce its head direction and maintain the crowd's centre of mass, but also to avoid other crowd member's positions. Equation 17 describes this force.

$$\vec{f}_p(t) = \vec{f}_p^{vis}(t) + \vec{f}_p^{att}(t) + \vec{f}_p^{rep}(t) \quad (17)$$

In order to maximize communication when walking in crowd, individual  $p$  at time  $t$  turns his vision direction to capture their members. Thus,  $\vec{f}_p^{vis}(t)$  vision force is included to help individual  $p$

adjust position to reduce head rotation. At the same time, individual  $p$  keeps a certain distance from the crowd's centre of mass by the force  $\vec{f}_p^{att}(t)$ . A repulsive force  $\vec{f}_p^{rep}(t)$  is added to support pedestrian  $p$  to avoid other crowd members.

In reality, the formation of small crowd varies from V-line, U-like, line-abreast, to river-abreast (Helbing, 2005). By tuning parameters of  $\vec{f}_p^{vis}$ , this model produces successfully these formations. By forcing members to follow a crowd's centre point, the study investigated the impact of crowd's population on crowd speed movement. It found that increasing crowd's population size decreased crowd's average speed.

However, the study only investigated a small crowd of up to four members while actual crowds in sport-like events may contain larger crowds. While social studies find that a crowd often contains more than one group and members of each group tend to stay together, this study only investigated a small size of a homogeneous crowd without investigating the interaction of members from different groups. Therefore, investigating the impact of a crowd that contains more than one group on crowd movement is necessary.

In comparison with CA-based and agent-based approaches, force-based approaches are potential to produce the emergence of self-organization phenomena of human crowds (Hoogendoorn, 2013). Therefore, the research of this thesis applied force-based approaches to understand the formation of groups in inhomogeneous crowds.

### 3 Research Questions and Methodology

Evidence from previous reports of emergency situations and dense places in Section 2.1.2 showed that crowds often consist of individuals from different social groups. Social studies investigating crowds highlight that individuals prefer to stay close to people who are familiar in order to maximize communication and reduce stress during emergency situations. Consequently, clusters emerge in inhomogeneous crowds as spatial coherence. The state of the art in modelling studies, presented in Section 2.3, have mostly investigated individual and following behaviours, but these behaviours typically occur in emergency situations. The research of this thesis investigates grouping behaviour because this behaviour is applicable to be occurred in both normal and emergency stations. As discussed in Chapter 2, how groups in crowds interact with each other has rarely been investigated. Exploring the emergence of clusters in inhomogeneous crowds becomes important to examine the impact of grouping behaviour on crowd movement. Therefore, this study defines two following research questions to explore the effect of grouping.

#### 3.1. Research Questions

**Question 1:** How to model the existence of groups and their impact on behaviour of individuals?

**Question 2:** What group-level behaviours, specifically clustering, emerge from the model?

The first question aims to model the interaction between individuals in crowds that contain different groups. Afterwards, the proposed model is applied to investigate the emergence of clusters in inhomogeneous crowds in typical floor plan layouts. This task aims to resolve the latter question.

#### 3.2. Research Methodology

This research is framed by the *design science* methodology, in comparison to research in other fields such as social science and political science that often rely on *behavioural science* and *participatory science*. While the later science paradigms explore “what is true”, *design science* focuses instead on “what is effective” (Hevner, 2004). The two main activities during the research are building artefacts and subsequently evaluate them. This research focuses on building a mathematical model and applying it to evaluate the effect of grouping behaviour in simulation environment of evacuation scenarios. There are additional research activities introduced in a design science framework including *theorising about* and *justifying* the artefacts (March and Smith, 1995). Theorising is used to describe “the construction of theories that explain how or why something happens”. (March and Smith, 1995).

This research study theorises the impact of grouping behaviour on crowd movement, by comparing the simulations of grouping behaviour to those of non-grouping behaviour. This study conducts metrics to perform the comparison and subsequently explains the impact. Although out of the scope of this study, justifying theory will further require actual data acquisition to calibrate the proposed model and subsequently validate it.

**Table 2** – The main artefacts being designed during this research, the table adapted from (March and Smith, 1995)

		Research Activities			
		Build	Evaluate	Theorise	Justify
Research Outputs	Constructs				
	Model	✓	✓		
	Method	✓	✓	✓	
	Instantiation	✓	✓		

Table 2 shows a matrix that defines the research activities and outputs which can be carried during a research. Ticked cells represents artefacts that will be produced in this research. The following paragraphs align the artefacts in the design science context to this research and describe what this research expects to produce in each corresponding artefact.

***Building the Construction*** In the design science paradigm, *constructs* provide supports to define and communicate problems and their solutions (Schon, 1983). Human crowd modelling approaches, which have been introduced in previous chapter, can be performed by various approaches ranging from defining agent’s behaviours rules to formulating social interaction forces. This research follows force-based approach and uses social forces to define the interaction between individuals in homogeneous and inhomogeneous crowds. The approach is chosen because it is simple and has been considered as sufficient to simulate commonly observable human crowd’s phenomena (Hoogendoorn, 2013).

***Building the Model*** A model is a “set of proposition or statement expressing relationships among constructs” (March and Smith, 1995). This study extends a force-based model that presents grouping behaviour of individuals in a homogeneous crowd (Mogilner, Edelstein-Keshet, 2003). In such homogeneous crowd, individuals are mutually attracted to each other. The base model has been used widely for modelling other systems including self-propelled particles, schooling fish, and other living organisms (Viscido, 2005; Orsogna, 2006; Johnson, 2008; Lukeman, 2010). Chapter 4 details the base model. The simulation of the model is observed to evaluate whether the movement

of individuals in such homogeneous crowds is similar with the description of grouping behaviour in reality.

The focus of this study is on inhomogeneous crowds that contain more than one group. Research Question 1 focuses on how to build a model that can reasonably formulate grouping behaviour in such crowds. The base model is extended to present the existence of groups in such inhomogeneous crowds. A new parameter is integrated into the base model to allow individuals differentiate in-group and out-of-group interactions. The extended model does not change the force calculating mechanism of the base model. It is subsequently evaluated by tuning the additional parameter to verify its sufficiency when simulating grouping behaviour in inhomogeneous crowds. It is expected to present the emergence of clusters in simulations when simulating such crowds.

***Evaluating the Model*** The homogeneity of clusters formatted in inhomogeneous crowds is measured to explore how individuals interact with in-group and out-of-group members. Chapter 5 addresses this research question.

***Building the Method*** A method is a “set of steps or an algorithm used to perform a task” (March and Smith, 1995). To investigate grouping behaviour in evacuation simulation scenarios, this study defines targets such as exiting doors to allow individuals in such inhomogeneous crowds move forward to reach the targets. This study develops a comparison between grouping and non-grouping behaviour to investigate the effect of grouping in crowd movement. Non-grouping behaviour formulates the asymmetrical attraction of individuals in crowds. Chapter 6 resolves the second research question. Section 6.1 develops an algorithm to present the symmetrical attraction.

***Instantiating the Method*** In design science framework, it is important to prove that an artefact is able to be implemented in a working system (Hevner, 2004). In this study, the comparison between grouping and non-grouping behaviours is deployed through simulation environments. Monash Cluster Campus facility is employed to perform parallel simulations. Four floor plans are constructed to simulate crowd evacuation scenarios. These floor plans are narrowing corridor, turning corridor, T-intersection corridor, and corridor with obstacle in the middle. They have been used widely in previous studies to investigate crowd dynamics (Helbing, 2002; Moussaid, 2011).

***Evaluating the Method and Instantiation*** Once non-grouping behaviour is developed, this study proposes metrics to conduct the comparison. The flow rates of these two behaviours are compared in typical floor plans to explore the effectiveness of the emergence of clusters in crowd movement. Other metrics, used in this study, are flowrate percentage difference, turning angles of



crowds during movement, and networks of individuals' strongest attractors. These metrics are applied to analyse the difference in flowrates of the two behaviours in typical floor plans. At the time when this study is undertaken, previous human crowd modelling studies have not provided a list of measurements to evaluate the grouping behaviour. Therefore, this study expects the proposed metrics will become a good reference resource for future studies. Section 6.2 presents these metrics. Proposed metrics are implemented to measure real-time simulations. Section 6.3 presents source codes developed to perform simulations. Simulation videos of the behaviours are also attached in the section. At the time when this research is taken, human crowd modelling studies do not have a public source code simulating grouping behaviour. Therefore, this study expects the simulation source code will become a reference for future studies.

***Theorising about the Method*** The final stage of this research is to theorise the effect of grouping in crowd movement. Section 6.4 investigates forces affecting on each individual in inhomogeneous crowds when they are grouping to their groups. It aims to explain how the emergence of clusters caused by grouping behaviour is effective in comparison with the emergence of crowds caused by non-grouping behaviour.

## 4 Modelling the Grouping Behaviour of Individuals in a Homogeneous Crowd

This chapter introduces a base model that is then applied to resolve the proposed research questions. The model is another version of force-based models, but it specialises to present the grouping behaviour of individuals in a homogeneous crowd (Mogilner, Edelstein-Keshet, 2003).

The model assumes that individuals in a homogeneous crowd prefer to stay together and avoid dispersion. When individuals are far from each other, they speed up from distant positions and slow down when they are closer.

The outcome of the model is that individuals keep a well-spaced distance from each other to avoid overlap at a state of equilibrium. A tight cluster of the crowd is formed at that state. This formation also maintains equidistant space for separation when the number of individuals in the crowd increases. Such equidistant space is not only observed in human groups but also in other ecological systems, such as flocks of gulls, anchovy schools, sandhill cranes, whenever a crowd is sedentary or moving in the same environmental conditions (Mogilner, 2003).

Given an individual  $p$  in a homogeneous crowd, the total interaction force acting on individual  $p$  is caused by other individuals  $q$ . Equation 18 presents the acceleration of individual  $p$  based on the force.

$$\frac{dv_p}{dt} = f(X_p, t) = \sum_{q(\neq p)} \vec{f}_{qp}(t) \quad (18)$$

The interaction force of an individual  $q$  acting on individual  $p$  is presented by using exponential functions. The force is denoted as  $\vec{f}_{qp}(t)$  and formulated using Equation 19.

$$\vec{f}_{qp}(t) = \left( Re^{\left(-\frac{|x(t)|}{r}\right)} - Ae^{\left(-\frac{|x(t)|}{a}\right)} \right) \vec{u}_{qp} \quad (19)$$

where

$R, r$	Magnitude, respectively range of repulsive force
$A, a$	Magnitude, respectively range of attractive force
$x$	Distance between individuals $q$ and $p$ at time $t$
$\vec{u}_{qp}$	Unit vector point from pedestrian $q$ to pedestrian $p$

The parameters,  $\mathbf{R}$ ,  $\mathbf{r}$ ,  $\mathbf{A}$ , and  $\mathbf{a}$ , are constant according to the model's parameter setting. In contrast, the distance  $x$  is changeable over time based on the distance between the individuals.

Parameters  $\mathbf{R}$  and  $\mathbf{A}$  present the magnitudes of repulsive and attractive forces respectively. Range parameters,  $\mathbf{r}$  and  $\mathbf{a}$ , present how fast their corresponding forces increase according to the distance

$x$ . Given a system of two individuals moving to each other in one dimensional space as shown in Figure 11, parameter pairs  $(R, A)$  and  $(r, a)$  are controlled such that the individuals perform grouping behaviour and the distance  $x > 0$  when the repulsion and the attraction are equal to each other.

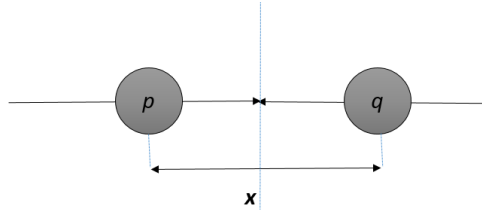


**Figure 11.** A two- individual system in one dimensional space

An online simulation of this system can be viewed at  
[https://sites.google.com/site/vietquangvo/home#1d\\_system](https://sites.google.com/site/vietquangvo/home#1d_system)

The condition  $(R > A \text{ and } r > a)$  is necessary such that individuals move close to each other and maintain a minimal separation distance at the state of equilibrium. Figure 12 explains why this condition is essential for grouping behaviour. In this figure, the change of the distance  $x$  is examined according to basic settings, which are  $(R > A \text{ and } r > a)$ ,  $(R < A \text{ and } r < a)$ ,  $(R < A \text{ and } r > a)$ , and  $(R > A \text{ and } r < a)$ .

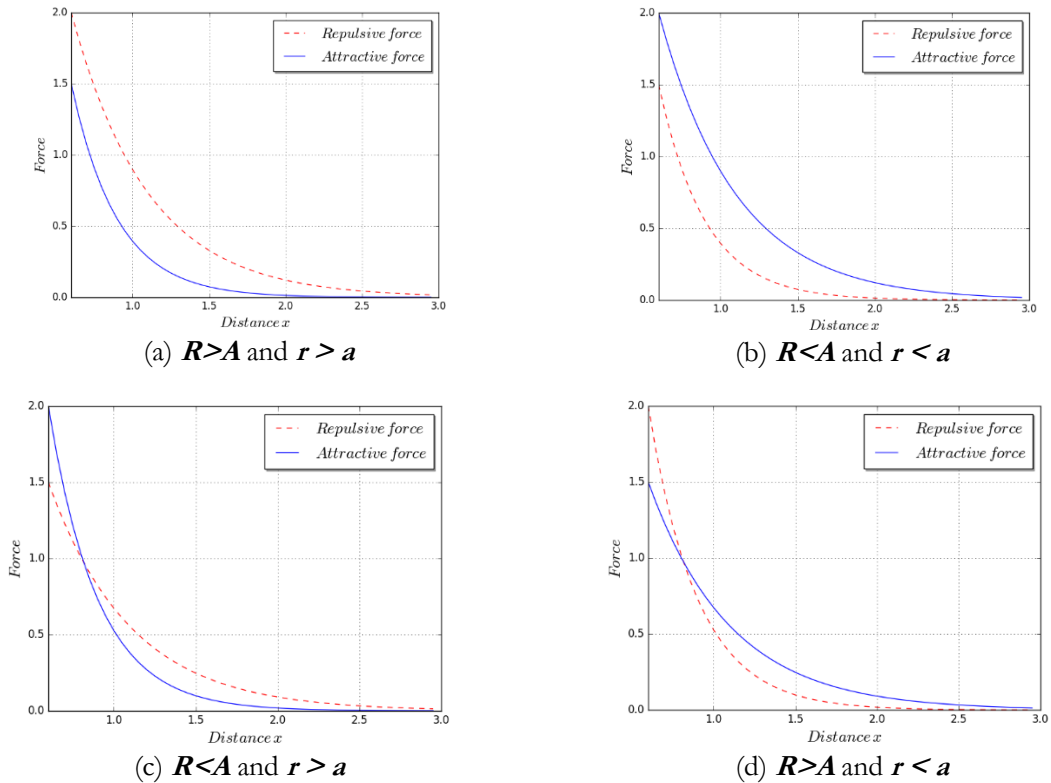


**Figure 12.** The distance between two individuals through parameter settings of base model

Figure 12.a presents the distance  $x$  when setting  $R > A$  and  $r > a$ . It shows that the repulsive force dominates the attractive force. Therefore, individuals move away rather than move close to each other. For that reason, this setting is not suitable.

In contrast, Figure 12.b shows the domination of attractive force even when individuals collide at  $x=0$  by setting  $R < A$  and  $r < a$ . This setting explains that individuals continue to move towards each other despite the distance  $x=0$ . Therefore, this setting is unrealistic.

Figure 12.c describes the distance  $x$  when setting  $R < A$  and  $r > a$ . At this setting, the long range of repulsion  $r$  makes individuals move away from each other when the distance  $x$  is large, while attractive force represses repulsive force when  $x \leq 0$ . Thus, this setting is not capable of presenting grouping behaviour that exhibits a distance  $x > 0$  to when individuals maintain a space for separation.

Figure 12.d shows the last setting that represents  $R > A$  and  $r < a$ . At this setting, long range attraction makes individuals move close to each other. A certain minimal separation distance  $x > 0$  is maintained because of the domination of repulsion magnitude  $R$  and short-ranged repulsion  $r$ . In Figure 12.d, the separation distance is identified when attractive and repulsive forces cancel each other. At this separation distance, individuals stop moving towards each other. This separation distance is called as comfortable distance  $\delta$ .

Validating the above parameter pairs concludes that the parameter setting ( $R > A$  and  $r < a$ ) is necessary for the base model to present the grouping behaviour of individuals in a homogeneous crowd. Other studies also verify that a short-range repulsion  $r$  and a longer-range attraction  $a$  are sufficient to generate observable movement patterns in animal groups (Katz, 2011).

The base model is a background of this research before extending into a further modelling step that focuses on inhomogeneous crowds. In essence, mathematical models need to be simulated to observe and explore how individuals in crowds behave dynamically. Therefore, this research applied Runge-Kutta level 4 numerical solver (RK4) to simulate the motion of individuals in a crowd over time (Fehlberg, 1969).

The RK4 method has been used widely to simulate particle systems and planets in universe due to the method's precision (Fehlberg, 1969). Given a particle that is at the position  $\vec{x}(t)$  and has the velocity  $\vec{v}(t)$  at time  $t$ , RK4 method approximates the new position  $\vec{x}(t + \Delta t)$  and the new velocity

$\vec{v}(t + \Delta t)$  at time  $(t + \Delta t)$  based on the force function  $f$  acting on that particle. Equation 20 presents the motion equation of the particle.

$$\begin{cases} \frac{d\vec{x}}{dt} = \vec{v} \\ \frac{d\vec{v}}{dt} = f(t, \vec{x}, \vec{v}) \end{cases} \quad (20)$$

In RK4 method, the new position  $\vec{x}(t + \Delta t)$  and the new velocity  $\vec{v}(t + \Delta t)$  is updated by the present position  $\vec{x}(t)$  and velocity  $\vec{v}(t)$  plus the weighted average of four increments. Each increment is the product of the time step  $\Delta t$ , and the corresponding slopes estimated from the system presented the Equation 20. Equations 21-26 summarise how to calculate  $\vec{x}(t + \Delta t)$  and  $\vec{v}(t + \Delta t)$ .

$$\vec{v}(t + \Delta t) = \vec{v}(t) + \frac{1}{6}(\vec{v}_{k_1} + 2\vec{v}_{k_2} + 2\vec{v}_{k_3} + \vec{v}_{k_4}) \quad (21)$$

$$\vec{x}(t + \Delta t) = \vec{x}(t) + \frac{1}{6}(\vec{x}_{k_1} + 2\vec{x}_{k_2} + 2\vec{x}_{k_3} + \vec{x}_{k_4}) \quad (22)$$

where

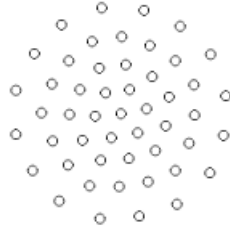
$$\begin{aligned} \vec{v}_{k_1} &= \Delta t f(t, \vec{x}_t, \vec{v}_t) \\ \vec{x}_{k_1} &= \Delta t \vec{v}_t \end{aligned} \quad (23)$$

$$\begin{aligned} \vec{v}_{k_2} &= \Delta t f(t + \frac{\Delta t}{2}, \vec{x}_t + \frac{1}{2}\vec{x}_{k_1}, \vec{v}_t + \frac{1}{2}\vec{v}_{k_1}) \\ \vec{x}_{k_2} &= \Delta t (\vec{v}_t + \frac{1}{2}\vec{v}_{k_1}) \end{aligned} \quad (24)$$

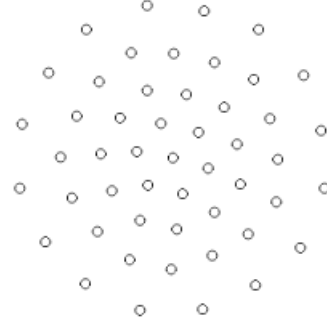
$$\begin{aligned} \vec{v}_{k_3} &= \Delta t f(t + \frac{\Delta t}{2}, \vec{x}_t + \frac{1}{2}\vec{x}_{k_2}, \vec{v}_t + \frac{1}{2}\vec{v}_{k_2}) \\ \vec{x}_{k_3} &= \Delta t (\vec{v}_t + \frac{1}{2}\vec{v}_{k_2}) \end{aligned} \quad (25)$$

$$\begin{aligned} \vec{v}_{k_4} &= \Delta t f(t + \Delta t, \vec{x}_t + \vec{x}_{k_3}, \vec{v}_t + \vec{v}_{k_3}) \\ \vec{x}_{k_4} &= \Delta t (\vec{v}_t + \vec{v}_{k_3}) \end{aligned} \quad (26)$$

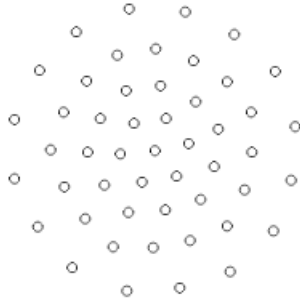
In this research, the base model was simulated to investigate how individuals behave in a homogeneous crowd by using RK4 method. Figure 13 shows different values of the comfortable distance  $\delta$ , which is the separation distance between individuals, at the state of equilibrium when setting with different combinations of parameters  $\mathbf{R}$  and  $\mathbf{A}$ .



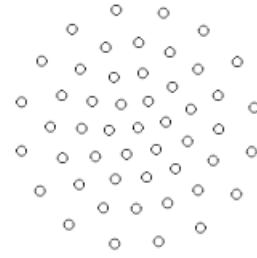
(a)  $\mathbf{R} = 35, \mathbf{A} = 20; \delta = 5.43$



(b)  $\mathbf{R} = 40, \mathbf{A} = 20; \delta = 8.25$



(c)  $\mathbf{R} = 35, \mathbf{A} = 18; \delta = 7.63$



(d)  $\mathbf{R} = 40, \mathbf{A} = 22; \delta = 6.36$

**Figure 13.** The comfortable distances  $\delta$  of a homogeneous crowd at different combinations  $(\mathbf{R}, \mathbf{A})$

Figure 13 shows the formation of a crowd containing  $\mathbf{N}=50$  individuals at the state of equilibrium at four different parameter combinations  $(\mathbf{R}, \mathbf{A})$ . The same settings for parameters  $\mathbf{r}$  and  $\mathbf{a}$  were used for the four cases:  $\mathbf{r} = 2.0$  and  $\mathbf{a} = 2.8$ . The increase of repulsive strength  $\mathbf{R}$  through Figures 13.a and 13.b generated a higher distance  $\delta$  between individuals. Particularly, the distance  $\delta$  increased from 5.43 to 8.25. This results conclude that the distance  $\delta$  is proportional to repulsive strength  $\mathbf{R}$ .

In Figures 13.a and 13.c, the distance  $\delta$  increased from 5.43 to 7.63 when parameter  $\mathbf{A}$  dropped from 20.0 to 18.0. On the other hand, the higher value of  $\mathbf{A}$  made individuals stay closer to form a tight cluster. In detail, this increase made  $\delta$  descend from 8.25 to 6.36 through Figures 13.b and 13.d. Therefore, this results shows the inverse proportion between  $\delta$  and attractive magnitude  $\mathbf{A}$ .

To summarise, this chapter introduces the base model that presents how individuals perform grouping in a homogeneous crowd. A tight cluster of the crowd is formed when individuals come

close to each other and maintain separation at the state of equilibrium. The condition ( $\mathbf{R} > \mathbf{A}$  and  $\mathbf{r} < \mathbf{a}$ ) is essential to simulate grouping behaviour that make individuals move close to each other and maintain a separated distance at the state of equilibrium. By using RK4 method to simulate the model, this research shows that the comfortable distance  $\delta$  is directly and inversely proportional to parameter  $\mathbf{R}$  and parameter  $\mathbf{A}$ , respectively. This chapter is an essential background before resolving the first question, which formulates the existence of groups in inhomogeneous crowds.

## 5 Modelling the Existence of Groups in An Inhomogeneous Crowd

This chapter addresses the first research question that focuses on how to model the existence of groups to form clusters in an inhomogeneous crowd. The base model, which was presented in Chapter 4, considers a homogeneous crowd in which all members of the crowd are equally attracted to each other. However, this research investigates inhomogeneous crowds that contain different groups. An individual in such an inhomogeneous crowd differentiates in-group and out-of-group interactions. This research aims to model how members of these different groups in the crowd behave dynamically and form clusters during crowd movement.

The modelling task is performed by using two steps. The first step, which is presented in Section 5.1, extends the base model to differentiate in-group and out-of-group interactions. The second step, which is presented in Section 5.2, is the integration of autonomous movement. The investigation of this model's behaviours in floor plan layouts is presented in the next chapter 6.

### 5.1. Modelling the Interaction between In-group Members and Out-of-group Members

In an inhomogeneous crowd, a group is a collection of individuals who have similar characteristics and tend to stay together while moving. A cluster is also a collection of individuals, however, it emerges spatially in the crowd because individuals of the same groups prefer to avoid out-of-group members. Social studies, which were presented in Section 2.1.2 of the Background Study Chapter, showed that members of the same group feel more familiar to stay together than staying in different groups. Consequently, clusters emerge as spatial coherence. Therefore, members of every group in an inhomogeneous crowd are modelled in the way that they are more repulsed by out-of-group members than in-group members. Moreover, members of a group are less attracted by out-of-group members than in-group members.

The base model, which was presented in Equation 19, integrates a new additional parameter  $c$  to present the interaction between members of different groups. In particular, Equations 27-28 presents the social force of individual  $q$  acting on individual  $p$ .



$$\vec{f}_{qp}(t) = \begin{cases} \left( Re\left(-\frac{|x|}{r}\right) - Ae\left(-\frac{|x|}{a}\right) \right) \vec{u}_{qp}, & \text{if } p, q \in \text{same group} \\ \left( \hat{R}e\left(-\frac{|x|}{r}\right) - \hat{A}e\left(-\frac{|x|}{a}\right) \right) \vec{u}_{qp}, & \text{if } p, q \notin \text{same group} \end{cases} \quad (27)$$

$$\text{where } \hat{R} = cR, \hat{A} = c^{-1}A; c \geq 1 \quad (28)$$

$R, r$	Magnitude, respectively range of repulsion for in-group member
$A, a$	Magnitude, respectively range of attraction for in-group member
$\hat{R}$	Magnitude of repulsion for out-of-group member
$\hat{A}$	Magnitude of attraction for out-of-group member
$c$	Relative strength of in-group and out-of-group interactions

The interaction force between individual  $q$  and individual  $p$  is computed through a condition using Equation 27. If individual  $q$  and individual  $p$  are in the same group, their interaction is based on repulsive magnitude  $R$  and attractive magnitude  $A$ . Otherwise, out-of-group repulsive magnitude  $\hat{R}$  and out-of-group attractive magnitude  $\hat{A}$  are used. Equation 28 presents the role of parameter  $c$ . The parameter increases the out-of-group repulsive magnitude  $\hat{R}$  and reduces out-of-group attractive magnitude  $\hat{A}$  based on magnitudes  $R$  and  $A$ .

To investigate whether the clusters emerging from the model's behaviour are consistent with the group membership, this study applied the purity measure (Amigo, 2009). The measure computes the homogeneity of clusters. Its value is always in the interval  $[0, 1]$ . High purity value means that groups in an inhomogeneous crowd are well separated. When purity value is equal to 1, individuals in such crowd are completely separated into clusters in which each cluster contains individuals that are from the same group. This measurement is described in Equation 29.

$$Purity = \frac{1}{N} \sum_{i=1}^K \max_j |c_i \cap g_j| \quad (29)$$

where

$N$	The number of individuals in the crowd
$K$	The number of clusters formed from the interaction of different groups
$c_i$	Cluster $i$
$g_j$	Group $j$

When parameter  $c=1$ , individuals do not differentiate in-group and out-of-group interactions since  $\hat{R} = cR$  and  $\hat{A} = c^{-1}A$ . Therefore, a tight cluster, which contains members of different groups, is formed at the state of equilibrium. Figure 14 shows this formation of groups in an inhomogeneous crowd.

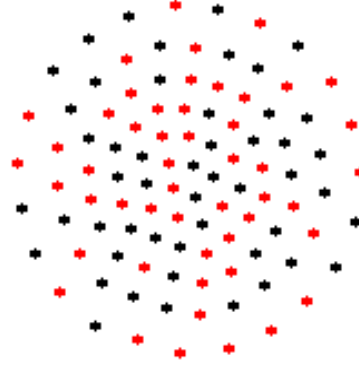


**Figure 14.** The formation of two groups in an inhomogeneous crowd when setting

$$A=20, R=40, c=1.0$$

Each group contained 50 members. At the state of equilibrium, the average distance between individuals was 8.4 and purity was 0.5 after simulated 20 times.

However, when  $c > 1$ , members of each group avoid out-of-group members while they are attracted by in-group members. Consequently, an inhomogeneous crowd forms clusters. Figure 15 shows instances of this formation when setting different values of parameter  $c$ .

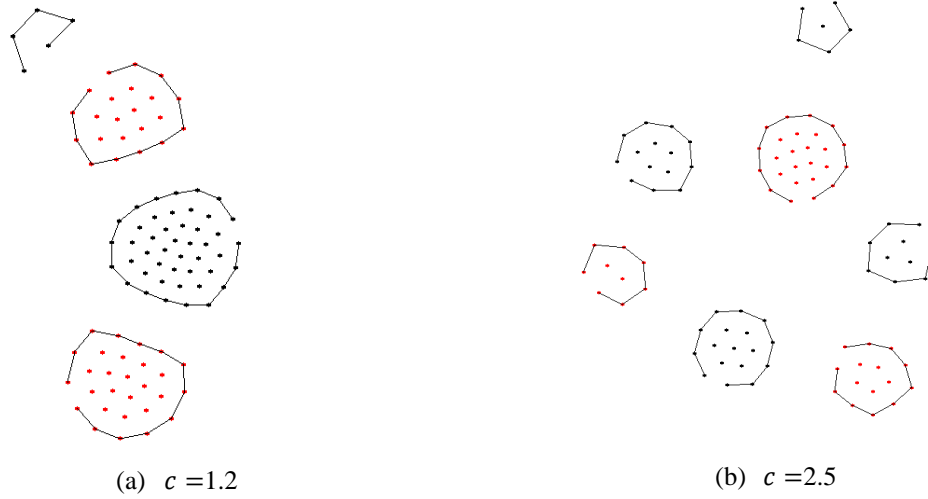


**Figure 15.** The formation of groups formed clusters

The simulation of clusters formed from different groups can be viewed at <https://sites.google.com/site/vietquangvo/home#groups>

The DBSCAN clustering algorithm was used to automatically detect clusters in inhomogeneous crowds. This algorithm is suitable for this analysis because it does not require the number of clusters in advance (Ester, 1996).

The Convex-hull algorithm is also used to detect individuals at the boundary of each cluster.

Figure 16 presents purity values for 27 representation parameter combinations ( $A, R, c$ ).

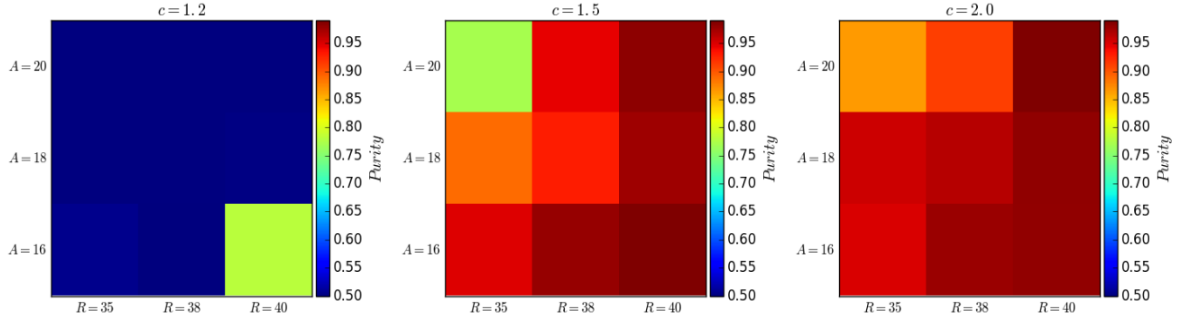


**Figure 16.** Purity measurement at different parameter combinations of  $(A, R, c)$

In Figure 16, the first subplot resulted when the setting was  $c = 1.2$ . The second and the last subplots were at  $c = 1.5$  and  $c = 2.0$ , respectively. Overall, the emerging clusters become increasingly purer with increasing  $c$  and increasing  $R$  because these parameters are proportional to the out-of-group interaction magnitude  $\hat{R}$ . In contrast, the increase of parameter  $A$  can potentially generate a lower purity when parameters  $c, R$  are at low values. However, the impact of parameter  $A$  on purity values decreases when parameters  $c$  and  $R$  at higher values.

To summarise, this research introduces a new parameter  $c, c > 1.0$ , to explain the separation of groups in inhomogeneous crowds through the formation of clusters. Higher values of parameters  $R$  and  $c$  make groups more separated. The purity of clusters in crowds can be controlled by parameters  $(A, R, c)$ .

## 5.2. Modelling Autonomous Movement of Individuals in a Crowd

This research uses target and obstacle forces to capture autonomous movement of individuals. These forces allow individuals to move towards a target, and to avoid obstacles. Figure 17 details all forces acting on an individual that causes its movement.

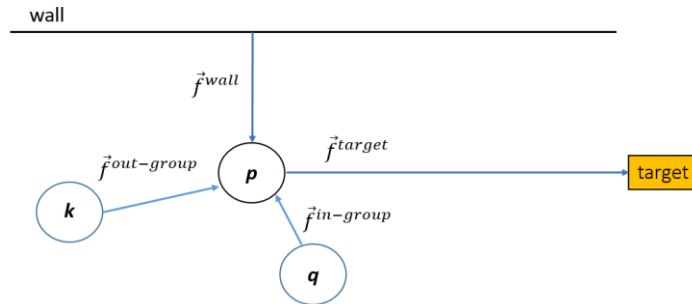


**Figure 17.** Social forces acting on individual  $p$

In Figure 17, individual  $p$  is attracted and repulsed by individual  $q$  and individual  $k$  respectively. In-group force is the sum of the forces caused by in-group members whereas out-of-group force is the sum of the forces caused by out-of-group members. Other forces, which are target and obstacle

forces, allow individual  $p$  to move towards the target and to avoid the wall. These social forces are formulated similarly with the interaction force between individuals based on their distance. Target force only has an attractive component to describe that each individual prefers to reach a specific target, such as an exit. This force has magnitude and a range of attraction. Obstacle force is caused by each wall or obstacle in floor plans. The force contains a magnitude and a range of repulsion to make individuals avoid that wall or obstacle.

Overall, the motion of individual  $p$ , which contains interaction forces, target force, and obstacle force, is given in Equations 30-33.

$$\frac{dv_p}{dt} = f(X_p, t) = \vec{f}^{target}(t) + \sum_{q(\neq p)} \vec{f}_{qp}(t) + \sum_w \vec{f}^{wall}(t) \quad (30)$$

$$\vec{f}^{target}(t) = -S e^{\left(-\frac{|d_{sp}(t)|}{s}\right)} \vec{u}_{sp} \quad (31)$$

where

$S, s$	Magnitude, respectively range of target force
$d_{sp}(t)$	Distance between target and pedestrian $p$ at time $t$
$\vec{u}_{sp}$	Vector point from target to pedestrian $p$

The target force  $\vec{f}^{target}$  is computed using the distance between individual and target. However, this study only considers the simplest form of the force that does not depend on the distance between individual and target to investigate the effect of grouping behaviour. This simple form is presented in Equation 32 and explains that all individuals have the same constant desire force to reach the target over time.

$$\vec{f}^{target}(t) = -S_{constant} \vec{u}_{sp} \quad (32)$$

The interaction force  $\vec{f}_{qp}$  between individual  $q$  and individual  $p$  is computed by using Equation 27-28. The obstacle force  $\vec{f}^{wall}$  is computed from the sum of walls of floor plan layouts using Equation 33.

$$\vec{f}^{wall}(t) = \widehat{W} e^{\left(-\frac{|d_{wp}(t)|}{\widehat{w}}\right)} \vec{u}_{wp} \quad (33)$$

where

$\widehat{W}, \widehat{w}$	Magnitude, respectively range of obstacle force
$d_{wp}(t)$	Distance between current wall $w$ and pedestrian $p$ at time $t$ . The distance is the length of the vector pointing perpendicularly from the individual's position to the wall's vector
$\vec{u}_{wp}$	Vector point from wall $w$ to pedestrian $p$

To summarise, an individual  $p$  is affected by the interaction force of in-group and out-of-group members, and subjected to additional forces comprising target and obstacle forces. The model is then used to investigate how groups interact in crowd movement.

## 6 The Emergence of Clusters in Crowd Movement

This chapter investigates the emergence of clusters from the interactions between individuals and groups in crowd movement. The model presented in the previous chapter is used for this investigation. Grouping and non-grouping behaviours are simulated to investigate which behaviour exhibits the emergence of clusters in different floor plans. The difference between the simulations of two behaviours is analysed to explore how the emergence of clusters is effective in crowd movement.

Section 6.1 describes how these behaviours were simulated differently using the model. Section 6.2 details floor plan layouts, and metrics to investigate the difference between the simulations of these behaviours. Sections 6.3 and 6.4 present and analyse the comparison results from the simulations of these behaviours, respectively.

### 6.1. Simulations of Grouping and Non-grouping Behaviours

The simulation of grouping behaviour contained different predefined groups in an inhomogeneous crowd. Grouping behaviour allowed individuals of the same group to move towards each other, and individuals of different groups to avoid each other. For instance, Figure 18 demonstrates grouping behaviour of individuals of the same group. Individuals contain bidirectional interactions when they are performing grouping behaviour.

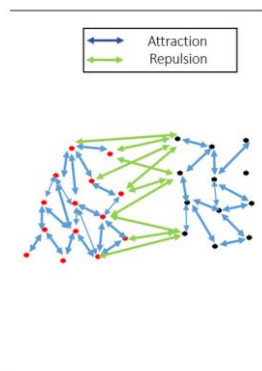


**Figure 18.** Grouping behaviour in a long corridor

The simulation was captured in a long corridor with setting  $A=2.0$ ,  $R=40$ , and  $c=1.4$ . The red and black colours signify group membership. The blue arrows represent the attraction of individuals in the same group. The green arrows shows the repulsion of individuals in different groups.

In contrast to the simulation of grouping behaviour, groups were not defined in the simulation of non-grouping behaviour. Non-grouping behaviour did not show bidirectional interactions between individuals in a crowd. Individuals selected and followed random attractors. For instance, Figure

19 shows non-grouping behaviour of individuals in a crowd in which they are not attracted mutually.

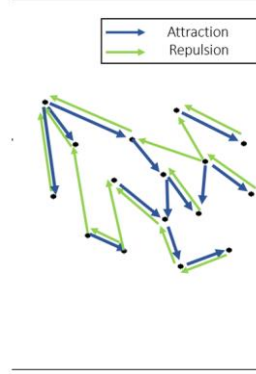


**Figure 19.** Non-grouping behaviour in a long corridor

The simulation was captured in a long corridor with setting  $A=2.0$ ,  $R=40$ , and  $c=1.4$ . Individuals are in the same black colour because of the nonexistence of groups. Individuals do not interact mutually with each other.

Overall, the difference between group and non-grouping behaviours was highlighted at the way individuals interact with each other. Grouping behaviour maintained bidirectional interactions between individuals, which were either in-group or out-of-group interactions, by defining groups. On the other hand, non-grouping behaviour showed unidirectional interactions between them and did not contain groups. Non-grouping behaviour made an attractor of an individual was not attracted symmetrically by that individual.

In order to focus on the investigation of the difference, other factors in the simulations of grouping and non-grouping behaviours needed to be the same. The model presented in Equation 30 shows that the motion of each individual depends on the interaction with in-group and out-of-group members. Therefore, the simulations of grouping and non-grouping behaviours needed to keep the same number of attractors for every individual over time. The following pseudocode details this condition, named *condition1*.

---

**Condition1:** The number of attractors of each individual

---

**Input:**

- i) Simulation at time  $t$
- ii) Crowd at time  $t$ ,  $C(t) = \{individual_1, \dots, individual_N\}$
- iii)  $s_1 \leftarrow$  Simulation of grouping behaviour of crowd  $C$
- iv)  $s_2 \leftarrow$  Simulation of non-grouping behaviour of crowd  $C$

**Output:** The number of attractors of every individual is the same for  $s_1$  and  $s_2$  over time  $t$

**Steps:**

- 1) **for each**  $individual_i \in C(t)$ :
  - 2)      $att_1 = \text{number\_of\_attractors}(individual_i, s_1)$
  - 3)      $att_2 = \text{number\_of\_attractors}(individual_i, s_2)$
  - 4)      $att_1 = att_2$
-

Moreover, the simulations of grouping and non-grouping behaviours were not limited at a finite number of individuals in a crowd. A constant flow of individuals was applied in the simulation of each behaviour. It aimed to ensure that every individual was attracted constantly to others who were in the front and behind them. Additional individuals were periodically generated to maintain a constant flow of an infinite number of individuals. The following algorithms present how to set attractors for each individual in the simulation of each behaviour over time. These algorithms were designed to maintain the *condition1*.

---

**Algorithm1:** The attractor setting for individuals in the simulation of grouping behaviour

---

**Input:** i) Simulation time  $t$ , simulation time step  $\Delta t > 0$

ii)  $k \leftarrow$  the number of groups in crowd

iii) Groups  $G = \{group_1, \dots, group_k\}$

iv) Crowd  $C(t=0) = \{individual_1, \dots, individual_N\}$

in which  $\begin{cases} \{individual_1, \dots, individual_{N/k}\} \in group_1 \\ \dots \\ \{individual_{(k-1)N/k}, \dots, individual_N\} \in group_k \end{cases}$

v)  $M \leftarrow$  list of additional individuals  $\{individual_1, \dots, individual_p\}$

**Output:** The number of individuals in  $C$  is increased by adding  $M$  periodically into groups  $G$   
The number of attractors of every individual is the same over time  $(t + \Delta t)$   
The symmetrical interactions between individuals are maintained in  $C(t + \Delta t)$

**Steps:**

- 1) while( $\Delta t > 0$ )
  - 2)     for each list of  $p/k$  individuals from  $M$
  - 3)         add this list into crowd  $C$  by assigning it to each group in  $G$
  - 4)         update attractors of individuals in each group in  $G$  from newly added individuals
  - 5)         update the number of individuals in  $C$  with  $N = N + p$
  - 6)      $t = t + \Delta t$
- 

The above algorithm presents the attractor setting for the simulation of grouping behaviour. For each time step  $\Delta t$ , a new additional individual in the list  $M$  receives  $N/k$  attractors. Due to the existence of groups in a crowd, individuals were mutually attracted and repulsed by in-group and out-of-group members, respectively. In this research, the simulation of grouping behaviour in the crowd of only one group was not considered. This case was not useful to investigate the emergence of clusters because a single group always forms a cluster. A singular group does not contain out-of-group interactions.

The following algorithm presents the attractor setting for the simulation of non-grouping behaviour. The algorithm creates asymmetrical interactions between individuals over time and

maintains the *condition1*. Specifically, the algorithm ensures that a new additional individual in the list  $\mathbf{M}$  receives  $N/k$  attractors for each time step  $\Delta t$ .

---

**Algorithm2:** The attractor setting for individuals in the simulation of non-grouping behaviour

---

**Input:**

- i) Simulation time  $t$ , simulation time step  $\Delta t > 0$
- ii)  $k \leftarrow$  the number of attractor to be assigned to every individual for each  $\Delta t$   
 $k$  is the same number with the number of groups in the simulation of grouping behaviour
- ii) Crowd  $\mathbf{C}(t=0) = \{\text{individual}_1, \dots, \text{individual}_N\}$   
in which each individuals has  $k$  random attractors from  $N$  individuals
- v)  $\mathbf{M} \leftarrow$  list of additional individuals  $\{\text{individual}_1, \dots, \text{individual}_p\}$

**Output:** The number of individuals in  $\mathbf{C}$  is increased by adding  $\mathbf{M}$  periodically into  $\mathbf{C}$   
The number of attractors of every individual is the same over time  $(t + \Delta t)$   
The asymmetrical interaction between individuals are maintained in  $\mathbf{C}(t + \Delta t)$

**Steps:**

- 1) while( $\Delta t > 0$ )
  - 2)     for each individual from  $\mathbf{M}$
  - 3)         add this individual into  $\mathbf{C}$   
              select randomly  $N/k$  attractors from  $\mathbf{C}$  for it  
              assign this individual as a new attractor for randomly  $N/k$  individuals from  $\mathbf{C}$
  - 4)     update the number of individuals in  $\mathbf{C}$  with  $N = N + p$
  - 5)      $t = t + \Delta t$
- 

To summarise, the proposed algorithms were used to simulate grouping and non-grouping behaviours. The simulation of grouping behaviour contained groups to present bidirectional interactions between individuals. The simulation of non-grouping behaviour did not contain groups. The simulations of grouping and non-grouping behaviour were performed and compared with different floor plans. The comparison aimed to investigate which behaviour exhibited the emergence of clusters and analyse its impact on crowd movement.

## 6.2. Floor Plans and Metrics for Investigating Grouping and Non-grouping Behaviours

The comparison between grouping and non-grouping behaviour was experimented with four commonly used floor plans, which are narrowing corridor, turning corridor, T-intersection corridor, and the corridor with obstacle. Figures 20-23 show these layouts. In each layout, shaded regions, marked by dashed lines, are the areas where individuals are generated periodically to create a constant flow of individuals.





**Figure 20.** Narrowing corridor

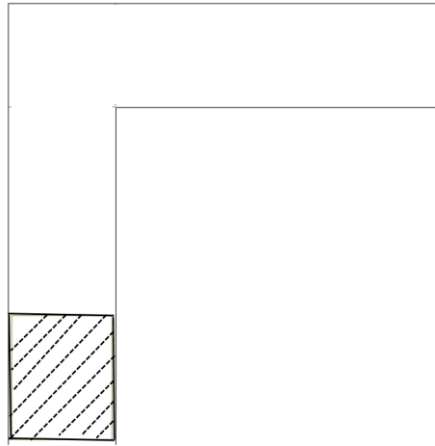


**Figure 21.** Turning corridor

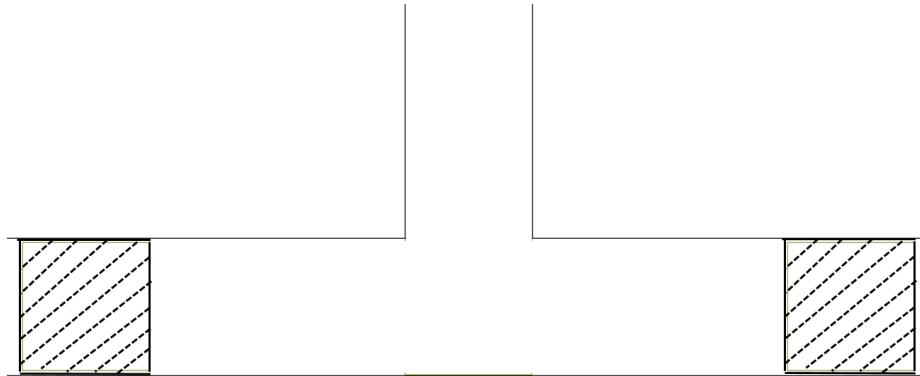


**Figure 22.** T-intersection



**Figure 23.** Corridor with obstacle

The results of the simulations of grouping and non-grouping behaviours were compared at different combinations of parameters ( $\mathbf{A}$ ,  $\mathbf{R}$ ,  $\mathbf{c}$ ). These parameters were employed because they reflect the strength of interaction forces between individuals. Each combination value of these

parameters was simulated fifty times. Monash Campus Cluster was occupied to perform parallel computations. However, each simulation was limited in a 120 second duration because the increase of the number of individuals over time and other computational tasks take more resources. Other parameters in the model were kept constant in the simulations,  $a=2.8$ ,  $r=2.0$ . These values were chosen because the constraint  $a > r$  presented in Chapter 4. The following metrics were used to analyse the difference between grouping and non-grouping behaviours.

- Flow rate distribution: Flow rate represents the average number of individuals exiting the floor plan per second. Flow rate distributions when simulating these two behaviours were compared by using the Man-Whitney  $u$ -test, which is a non-parametric hypothesis testing.
- The percentage flow rate difference,  $\Delta_{flowrate}$ : This metric aimed to identify which floor plan had the largest difference when simulating these two behaviours. It also allows to explore how the difference varied according to the combinations of parameters ( $A$ ,  $R$ ,  $c$ ).
- Turning angle distribution: Turning angle of each individual at time  $t$ ,  $\theta(t)$ , is the angle between velocity vector  $\vec{v}_i(t)$  and target vector  $\vec{v}_{ie}(t)$  pointing from the current position of that individual to a target point. Turning angle distribution comprises the turning angles of all individuals involved in fifty simulation trials for each behaviour. Kullback-Leiber (KL) distance was then computed to investigate how much the turning angle distributions of these behaviours differ.
- Network of the most influential attractors presents attractors that exert the strongest force of each individual over time. The networks of the simulations of these two behaviours were constructed to identify which behaviour made an individual switched fewer attractors over time.

### 6.3. Results of the Difference between Grouping and Non-grouping Behaviours

In this section, the comparison results between the simulations of grouping and non-grouping behaviours are presented for each floor plan. This work aims to explore which behaviour is consistently effective for crowd movement in both floor plans. The simulation source code and data visualisation used for this experiment can be downloaded at:

<https://github.com/vietvomonash/EffectofGrouping>

### 6.3.1. The Difference in Narrowing Corridor

Figure 24 shows the observation when simulating two behaviours with setting  $A = 20$ ,  $R = 40$ , and  $c = 1.4$ . Figure 24.a presents the movement caused by grouping behaviour. Figure 24.b shows the movement of non-grouping behaviour.

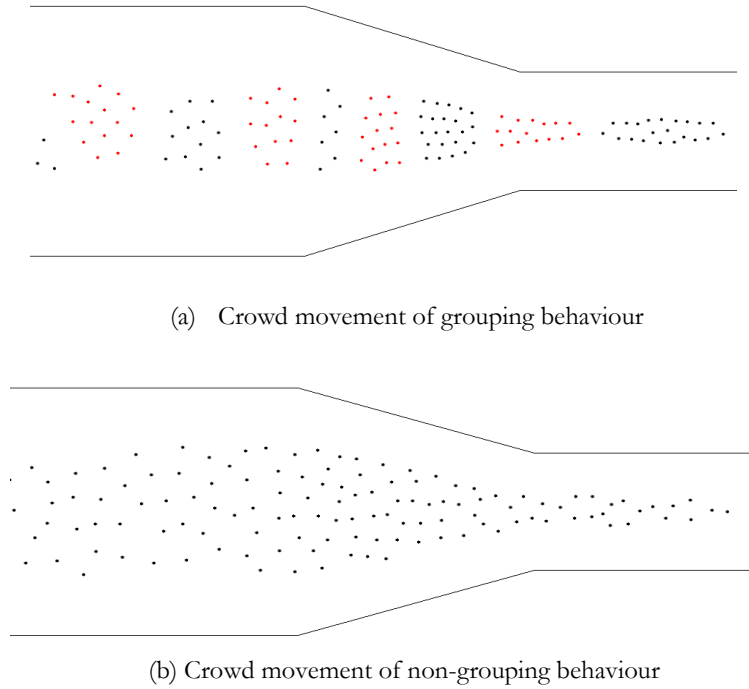


**Figure 24.** Observation of grouping and non-grouping behaviours in a narrowing corridor

Simulation videos of these behaviours in a narrowing corridor can be viewed at [https://sites.google.com/site/vietquangvo/home#narrowing\\_corridor](https://sites.google.com/site/vietquangvo/home#narrowing_corridor)

The colours signify group membership. In Figure 24.a, different groups are defined in the simulation of grouping behaviour. In contrast, groups are not defined in the simulation of non-grouping behaviour in Figure 24.b.

Figure 24.a shows clusters form from groups while Figure 24.b does not shows clusters. The simulations of grouping and non-grouping behaviours were monitored at different parameter combinations to compare their flow rates. Figure 25 presents the flow rate distributions at the 64 combinations of parameters ( $A$ ,  $R$ ,  $c$ ).

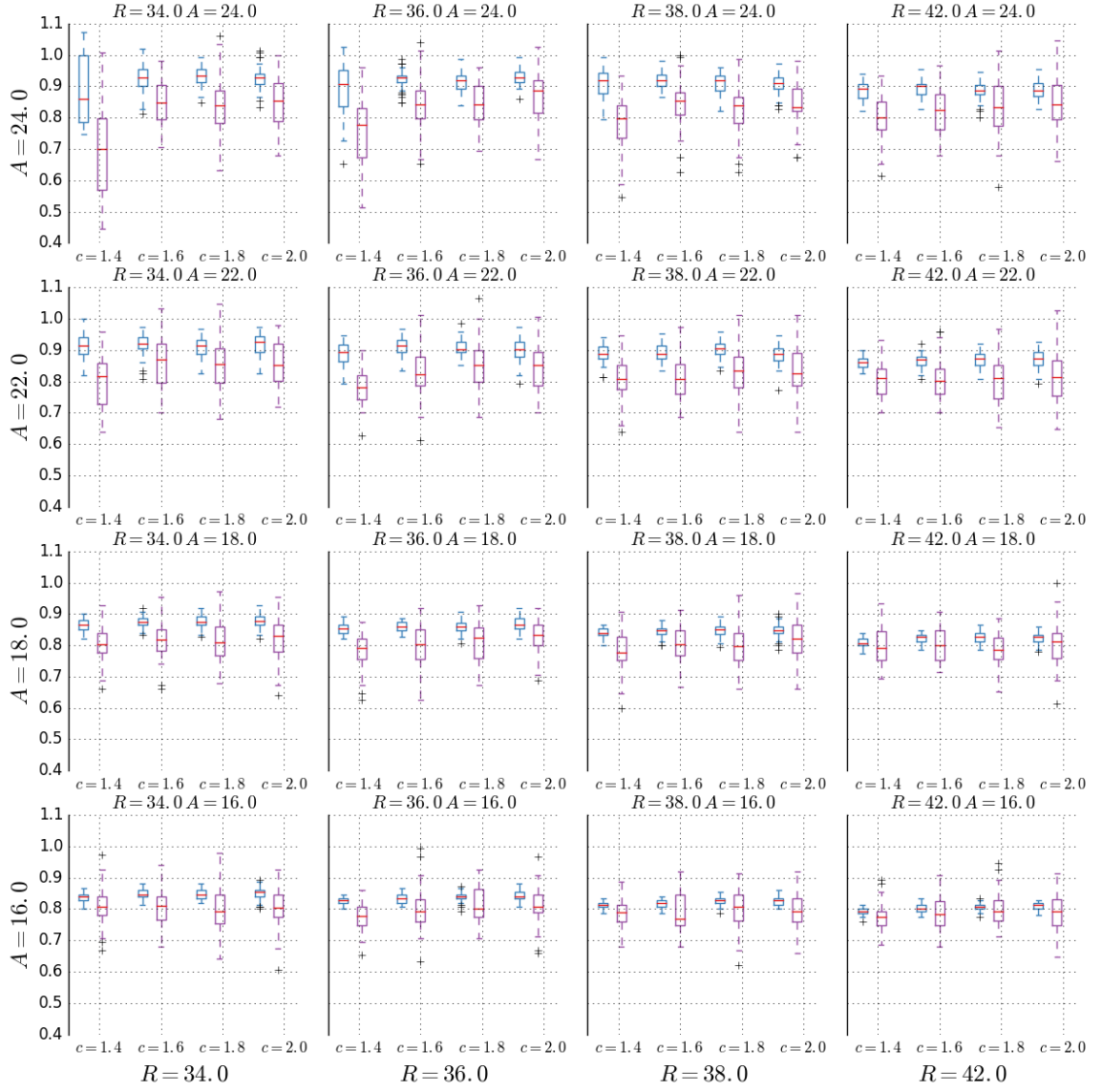


**Figure 25.** Flowrate distributions in the narrowing corridor

The blue colour presents the flowrate distributions of grouping behaviour while the red colour presents the distribution of non-grouping behaviour. Each row represents a certain value of parameter  $A$  while each column stands for a particular value of parameter  $R$ .

Overall, the flowrate of grouping behaviour was higher than the flow rate of non-grouping behaviour. For instance, at  $R=34.0$ ,  $A=24.0$ ,  $c = 1.4$ , the average flowrate of grouping behaviour was 0.85 while non-grouping only resulted at 0.7. All mean differences are significant at the 5% level. The flowrate percentage difference  $\Delta_{flowrate}$  of the behaviours were calculated in the heat map presented in Figure 26. In this figure, each subplot presents the difference at a certain value of parameter  $c$  of different combinations of  $A$  and  $R$ .

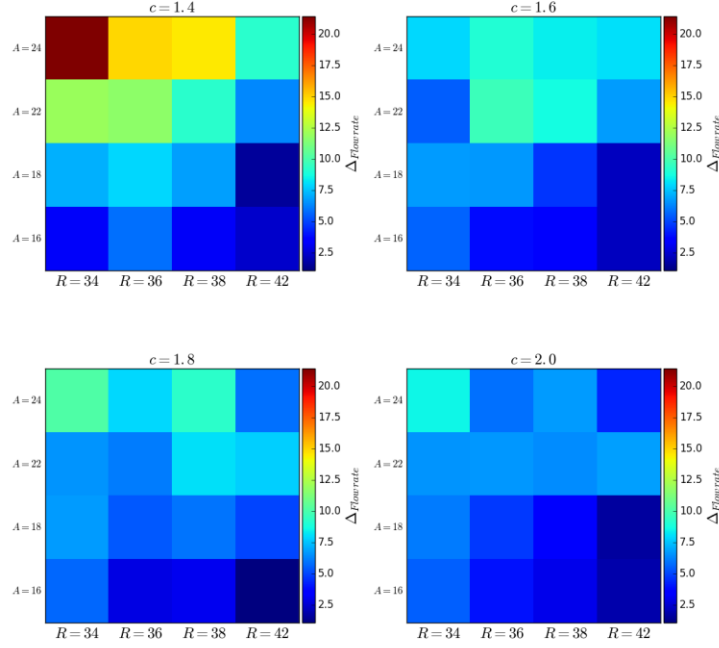


**Figure 26.** The heat map of the flowrate percentage difference in the narrowing corridor

The flowrate percentage difference varied in the range from 2.5% to 20%. The difference showed that grouping behaviour created significantly higher flow rates than non-grouping behaviour. At each value of parameter  $c$ , increasing attractive magnitude  $A$  makes  $\Delta_{flowrate}$  increase while the increase of repulsive strength  $R$  makes  $\Delta_{flowrate}$  descend. For instance, at  $c = 1.4$ ,  $\Delta_{flowrate}$  increased from 2.5 percent to 20.0 percent when attractive magnitude  $A$  increased from 16.0 to 24.0. In contrast, a decrease was observed from 5.0 to 2.5 percent when repulsive strength  $R$  increased from 34.0 to 42.0. The increase of parameter  $c$  makes the variation of  $\Delta_{flowrate}$  smaller. For example,  $\Delta_{flowrate}$  varied in the range of 2.5% to 20% at  $c = 1.4$ , while that value varied in the range 2.5 to 7.5% at  $c = 2.0$ .

To examine how the movement of individuals contributed to the difference in the flowrates of grouping and non-grouping behaviours, the movement of individuals were monitored over time by measuring their turning angles. Their turning angle distribution was then compared with a testing distribution. The testing distribution was extracted from the forward movement of a small crowd to exit a narrowing corridor. The angle  $\theta$  between velocity vector  $\vec{v}_i(t)$  and target vector  $\vec{v}_{ie}(t)$  of every individual was close to 0 degree. Figure 27 presents the turning angle and the testing distribution.

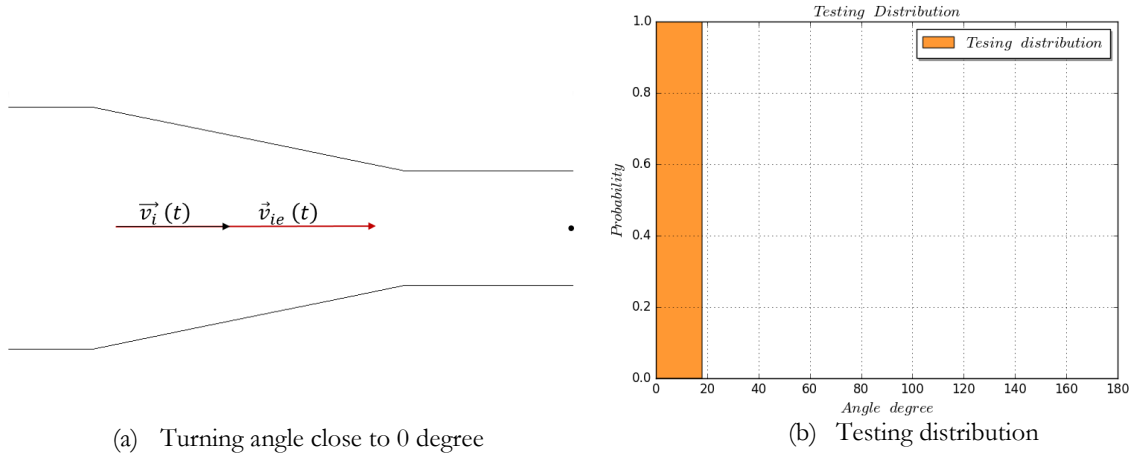


**Figure 27.** A testing distribution in the narrowing corridor

The Kullback-Leiber (KL) distance was then applied to measure the distance between the turning distribution of each behaviour and the testing distribution. For instance, Figure 28 presents the turning angle distributions when simulating two behaviours with setting  $A = 24$ ,  $R = 42$ ,  $c=1.4$ .

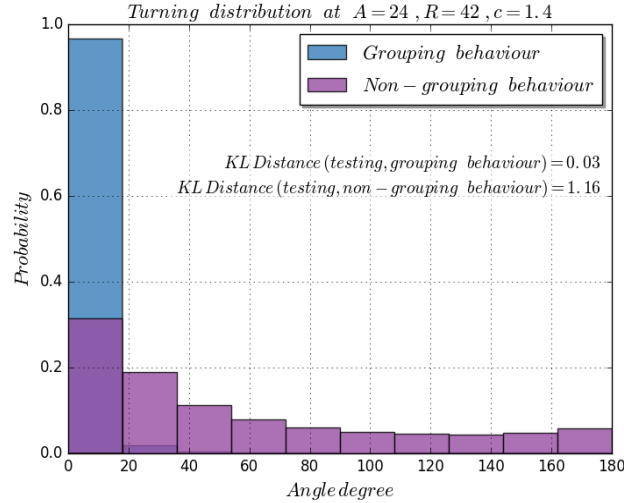


**Figure 28.** The turning angle distribution of grouping and non-grouping behaviours in the narrowing corridor

At this parameter combination, the turning angle distribution of grouping behaviour was almost the same with the testing distribution. The KL distance was calculated at 0.03. In contrast, angle degrees of non-grouping behaviour varied greatly from 0 degree to 180 degree. Noticeably, there were angle degrees at 160 to 180. These degrees confirmed that there was a number of individuals that moved backward instead of exiting the corridor. The KL distance of non-grouping behaviour was computed at 1.16, higher than the KL distance of grouping behaviour. This results showed that the movement of grouping and non-grouping behaviour was different. KL distances at other parameter combinations are shown in Figures 29-32. Each figure contains the heat map of KL distances at a certain value of parameter  $c$ .

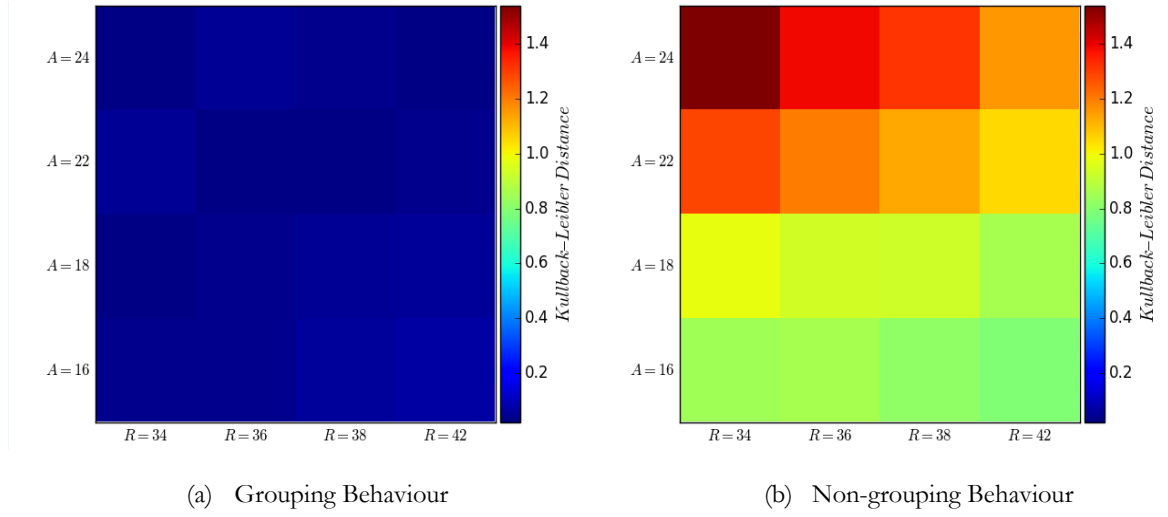


**Figure 29.** The heat map showing the KL distances in the narrowing corridor when setting  $c=1.4$

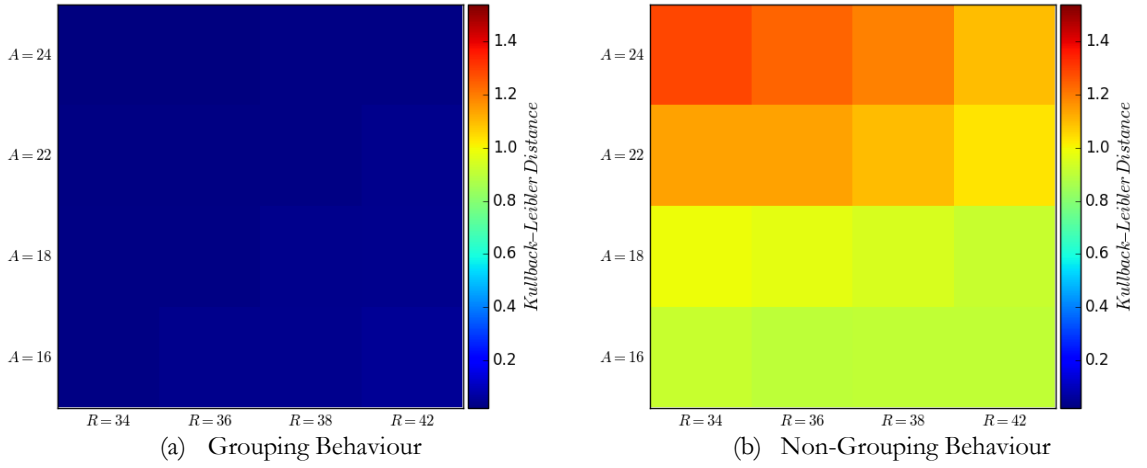


**Figure 30.** The heat map showing the KL distances in the narrowing corridor when setting  $c=1.6$

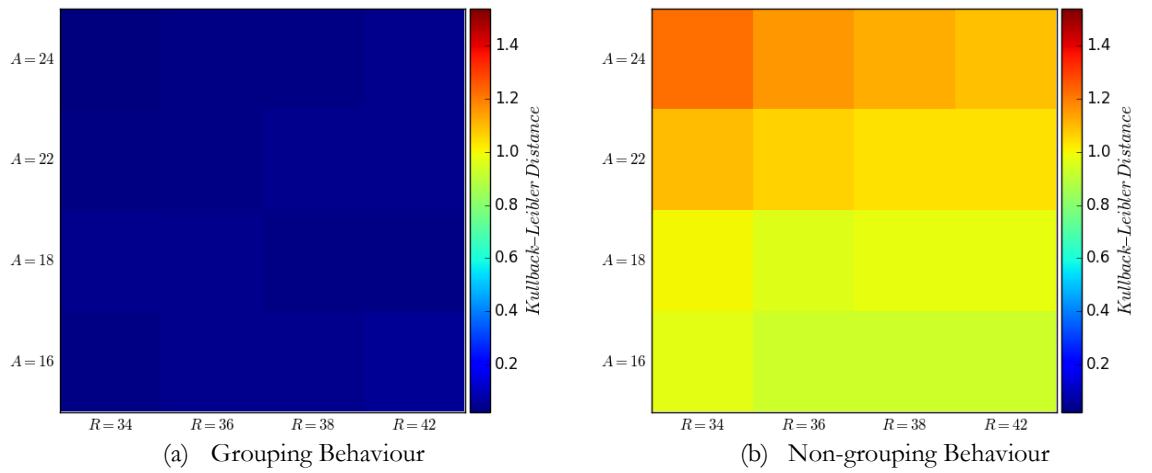


**Figure 31.** The heat map showing the KL distances in the narrowing corridor when setting  $c=1.8$

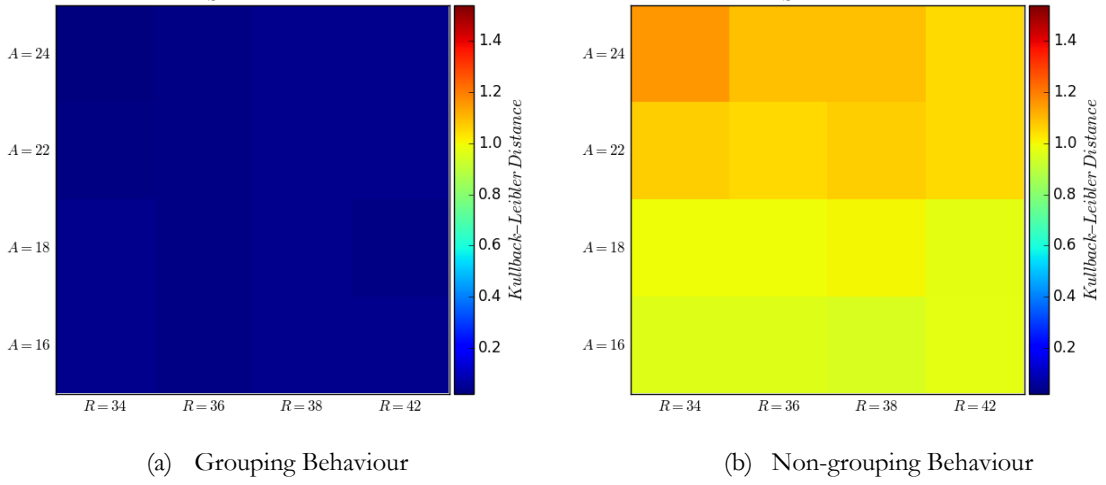


**Figure 32.** The heat map showing the KL distances in the narrowing corridor when setting  $c=2.0$

Overall, the turning distribution of grouping behaviour was different from the turning angle distribution of non-grouping behaviour. The KL distances of grouping behaviour was very low, around 0.2, across all parameter combinations. In contrast, the KL distances of non-grouping behaviour varied more greatly. Moreover, the increase of attractive magnitude  $A$  in the simulation of non-grouping behaviour created higher KL distances. This result showed that individuals' turning angles were more different from 0 degree, which stands for forward movement.

To investigate how individuals behaved in narrowing corridor, the network of the strongest attractors of each individual over time was constructed. Figure 33 shows the networks of the two behaviours. Each node in a network represents an individual. The degree of each node is equivalent to the number of times an individual switched its attractors.

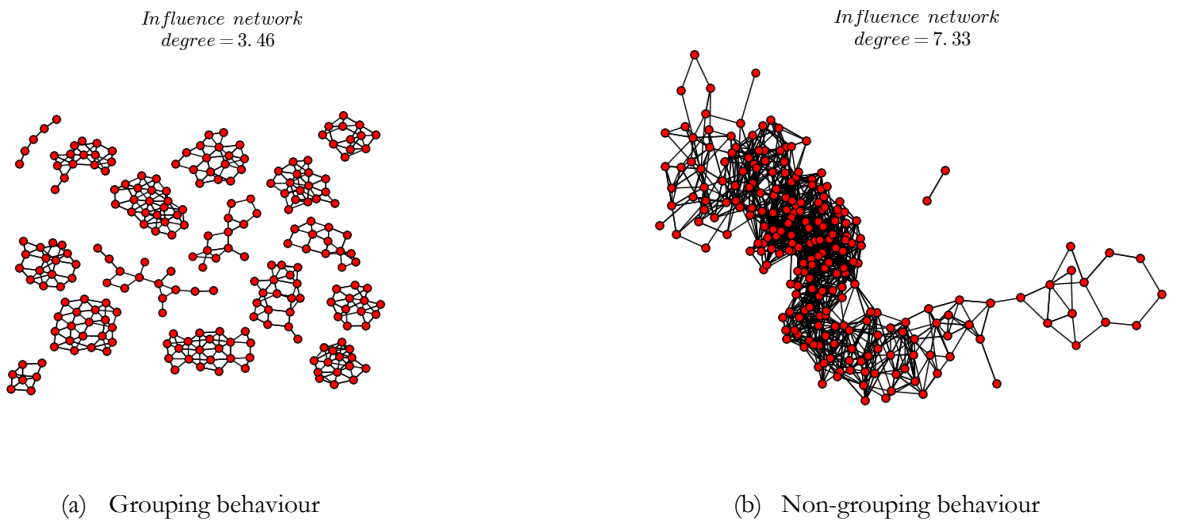


**Figure 33.** The influence networks of two behaviours in the narrowing corridor with setting

$$A=24.0, R = 34.0, \text{ and } c = 1.4$$

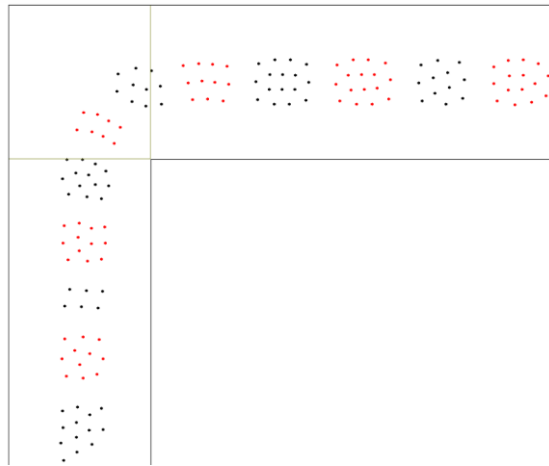


Figure 33 clearly shows that the network of grouping behaviour was seen in clusters. This results represented that individuals were in clusters to exit the narrowing corridor. An individual switched on average 3.46 attractors. In contrast, the network of non-grouping behaviour did not create clusters and its degree was significantly higher, at 7.33. The result showed that individuals switched more attractors during crowd movement of non-grouping scenario.

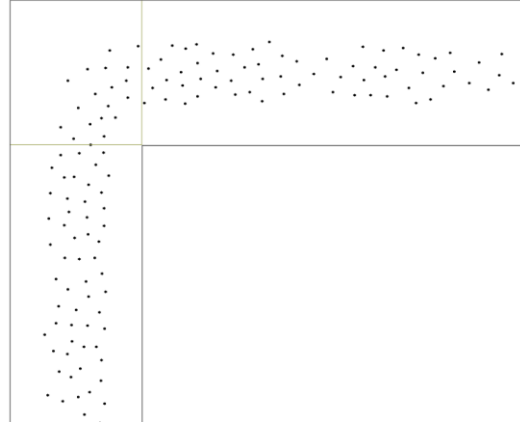
In general, the results from the proposed metrics in narrowing corridor showed that grouping behaviour was effective for crowd movement. When individuals performed grouping behaviour, clusters emerged and created an ordered movement. The emergence allowed individuals stay together with their in-group members while they are moving in the corridor. In contrast, non-grouping behaviour created turbulence because individuals move irrationally to re-arrange their crowd flow over time. Specifically, they frequently switch their attractors.

### 6.3.2. The Difference in Turning Corridor

This section presents the difference between grouping and non-grouping behaviours in a turning corridor. Figure 34 shows the simulation of these behaviours with setting  $A = 20$ ,  $R = 40$ , and  $c = 1.4$ . The observation of the simulation was similar to the observation in the narrowing corridor, clusters emerged when individuals mutually grouped to in-group members. In contrast, non-grouping behaviour did not show the emergence of clusters.



(a) The movement of grouping behaviour



(b) The movement of non-grouping behaviour

**Figure 34.** The observation of grouping and non-grouping behaviours in a turning corridor

Simulation videos of these behaviours in a turning corridor can be viewed at [https://sites.google.com/site/vietquangvo/home#turning\\_corridor](https://sites.google.com/site/vietquangvo/home#turning_corridor)

The flow rate distributions of two behaviours were monitored at the 64 combinations of parameters ( $A$ ,  $R$ ,  $c$ ). Figure 35 presents this result. In general, the flowrate of grouping behaviour was higher than the flow rate of non-grouping behaviour.

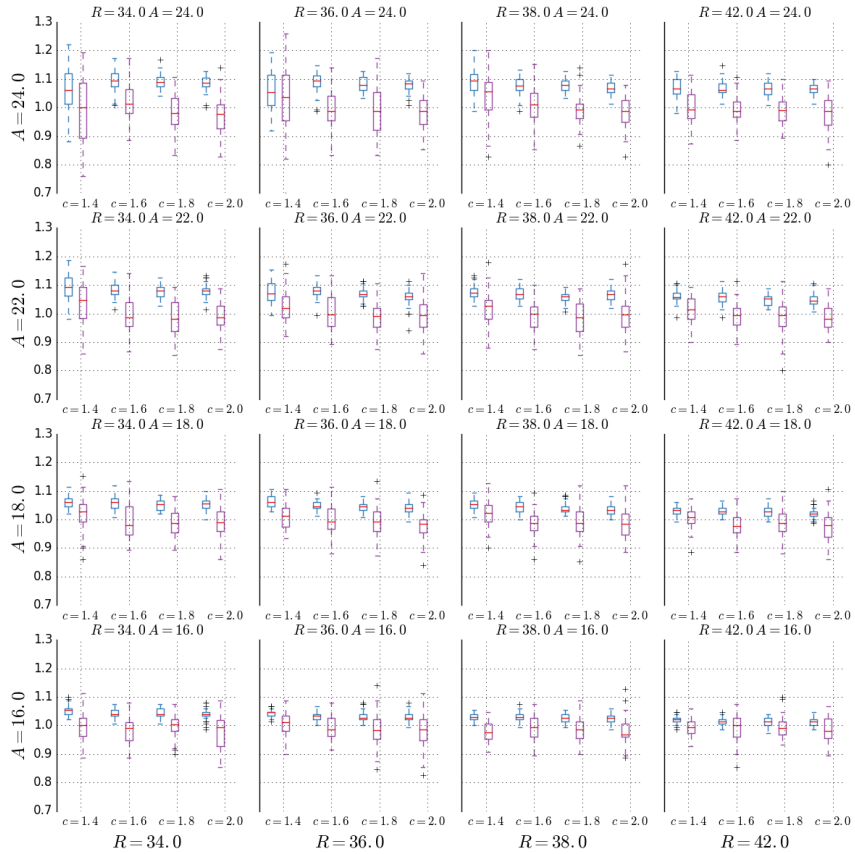


**Figure 35.** Flowrate distributions of two behaviours in the turning corridor

The blue colour presents the flowrate distributions of grouping behaviour while the red colour presents the distribution of non-grouping behaviour. Each row represents a certain value of parameter  $A$  while each column stands for a value of parameter  $R$ .

The flowrate percentage difference  $\Delta_{flowrate}$  of two behaviours were summarized in the heat map presented in Figure 36.

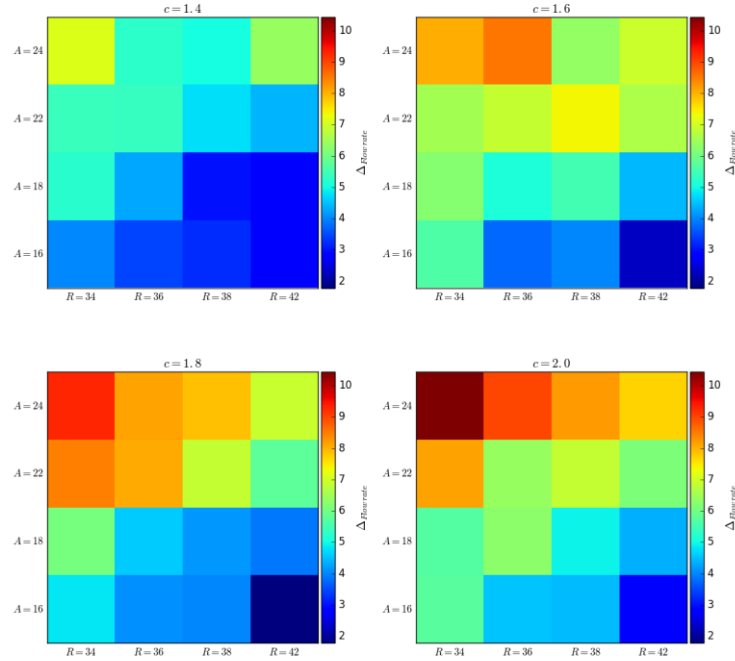


**Figure 36.** The heat map of the flowrate percentage difference in the turning corridor

Overall, the flowrate percentage difference varied in the range from 2% to 10%. The difference showed that grouping behaviour created significantly higher flow rates than non-grouping behaviour.

The testing distribution of a small crowd was obtained in Figure 37. The distribution contained turning angles in the range from 0 to 90 degree to describe turning movement.

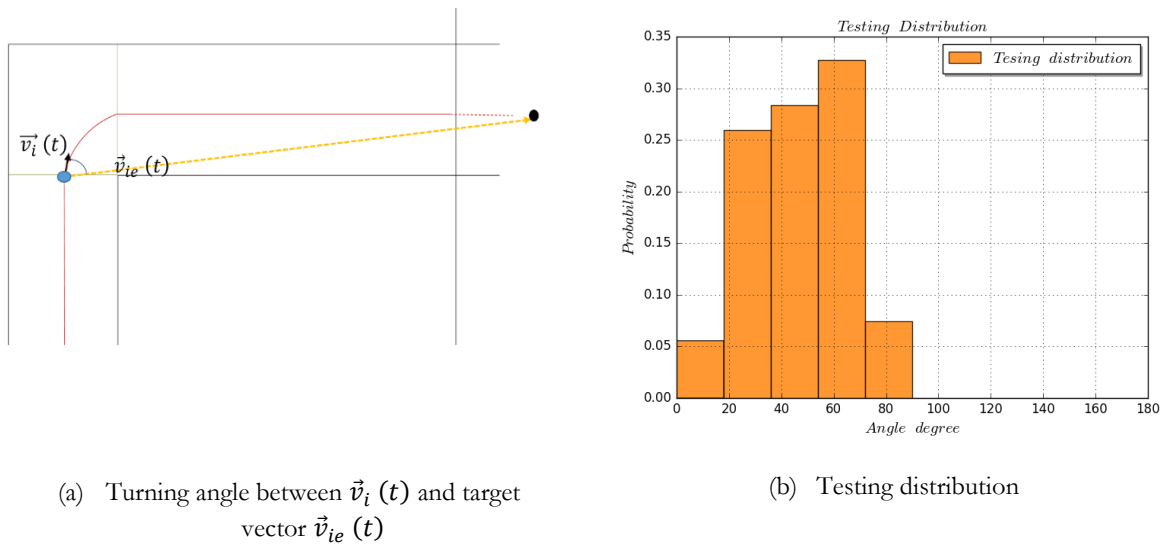


**Figure 37.** The testing distribution in the turning corridor

The KL distances between the turning angle distributions of each behaviour and the testing distribution were analysed to investigate how individuals moved in the turning corridor. Figures 38-41 presents the heat map of the KL distances of each behaviour.

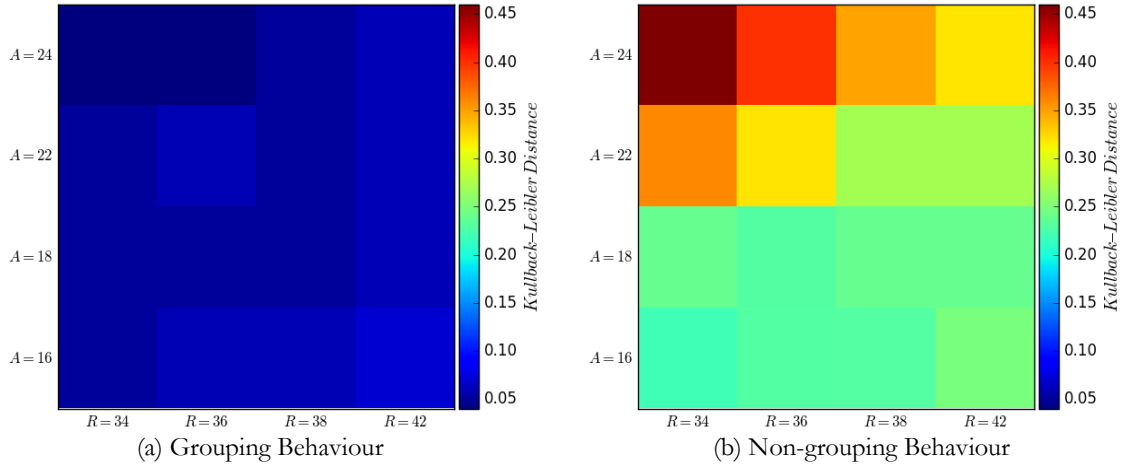


**Figure 38.** The heat map showing the KL distances in the turning corridor with setting  $c=1.4$

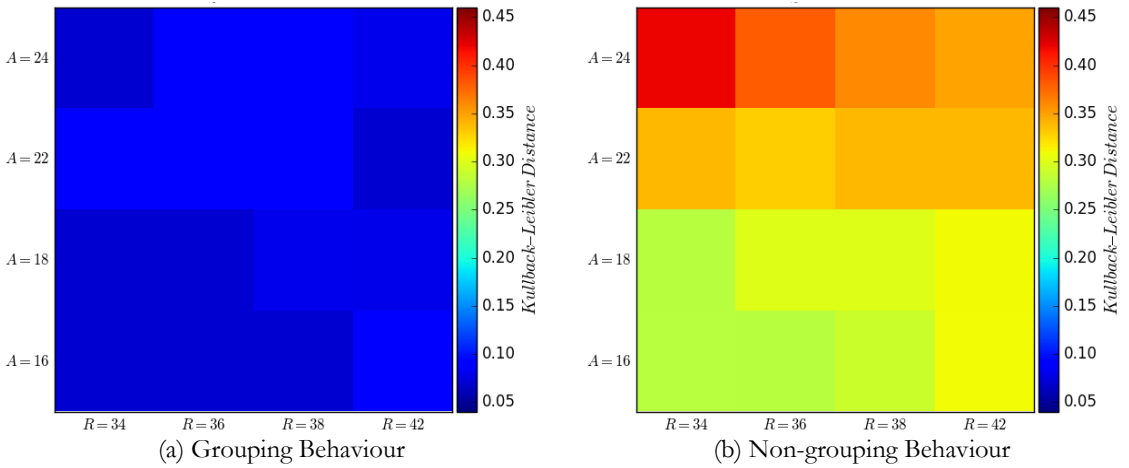


**Figure 39.** The heat map showing the KL distances in the turning corridor with setting  $c=1.6$

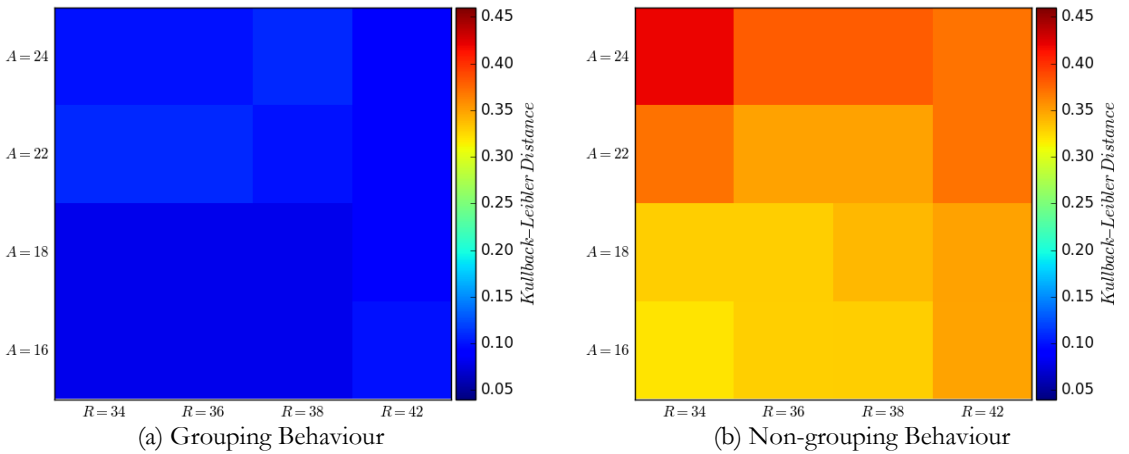


**Figure 40.** The heat map showing the KL distances in the turning corridor with setting  $c=1.8$

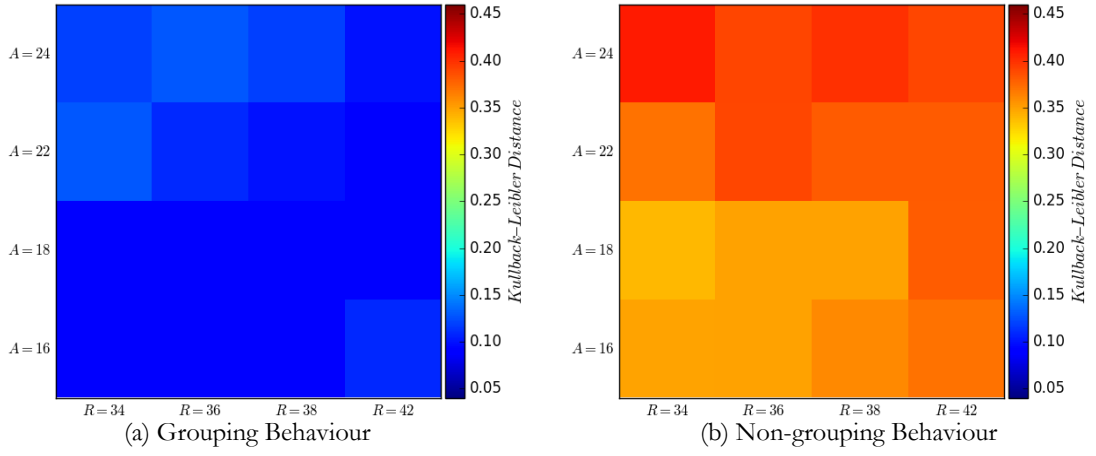


**Figure 41.** The heat map showing the KL distances in the turning corridor with setting  $c=2.0$

Overall, the turning angle distribution of grouping behaviour was almost the same with the testing distribution because their KL distances were very small at all parameter combinations. In contrast, the turning angle distribution of non-grouping behaviour were significantly different from the testing turning angle distribution. Moreover, the increase of attractive magnitude  $A$  in this scenario created higher KL distances. This result showed that a higher attractive magnitude made individuals moved more differently.

To investigate how individuals behaved in the corridor, the network of the strongest attractors of each individual over time was constructed. Figure 42 shows the networks of the simulations of grouping and non-grouping behaviours.

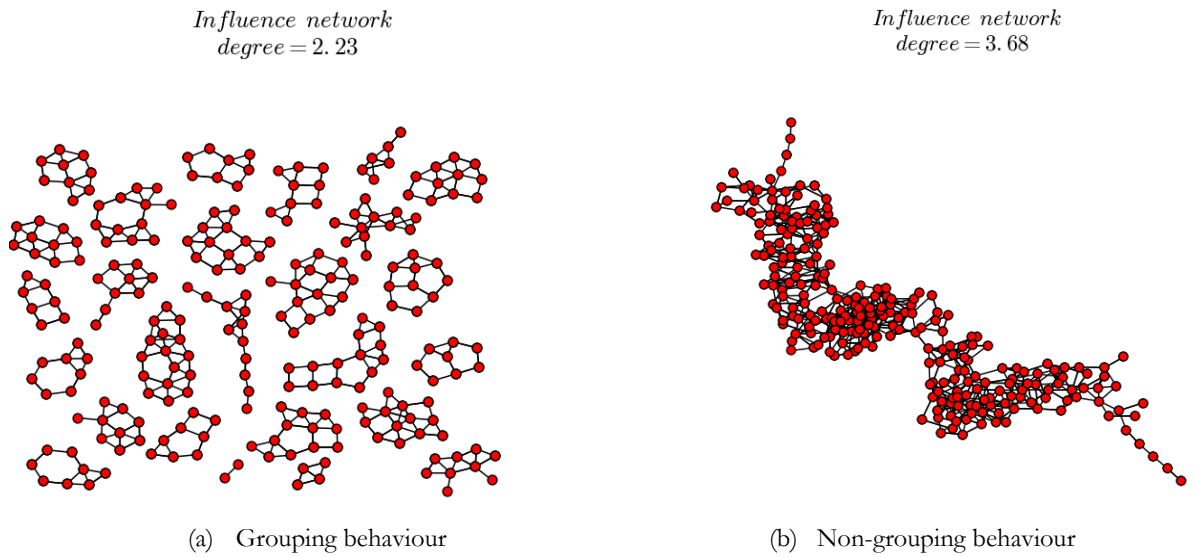


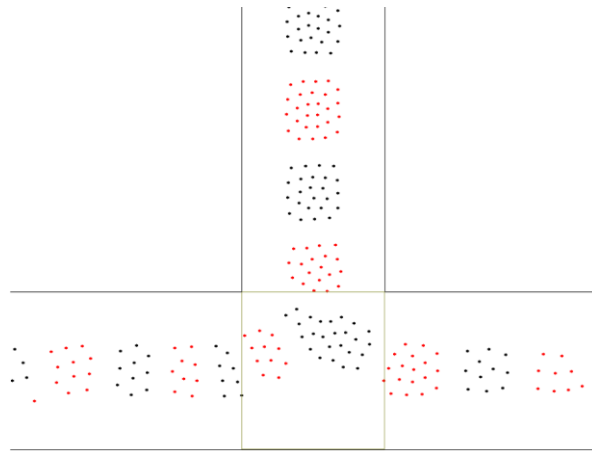
**Figure 42.** The influence networks of two behaviours in the turning corridor with setting

$$A=20.0, R=36.0, c = 1.4$$

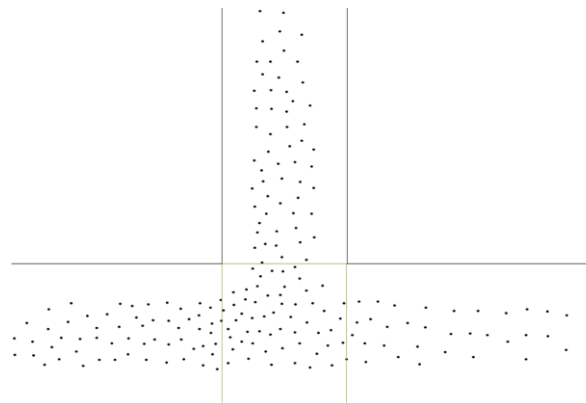
In the network of grouping behaviour, clusters were formed. This result showed that individuals were in clusters when they were moving to exit the turning corridor. An individual switched on average 2.23 attractors. In contrast, the degree in the network of non-grouping behaviour was significantly higher at 3.68. Clusters were not observed in this network. This result showed that the movement of non-grouping behaviour created turbulence.

### 6.3.3. The Difference in T-intersection Corridor

This section presents the difference between grouping and non-grouping behaviours in a T-intersection corridor. Figure 43 shows the simulations of the behaviours with setting  $A = 20$ ,  $R = 40$ , and  $c = 1.4$ .



(a) The movement of grouping behaviour



(b) The movement of non-grouping behaviour

**Figure 43.** The observation of grouping and non-grouping behaviours in a T-intersection corridor

Simulation videos of these behaviours in a T-intersection corridor can be viewed at [https://sites.google.com/site/vietquangvo/home#intersection\\_corridor](https://sites.google.com/site/vietquangvo/home#intersection_corridor)

Figure 43.a shows the emergence of clusters caused by grouping behaviour. In contrast, Figure 43.b does not show the emergence of clusters caused by non-grouping behaviour. Figure 44

presents the flow rate distributions when simulating each behaviour in the corridor at the 64 combinations of parameters ( $A$ ,  $R$ ,  $c$ ).

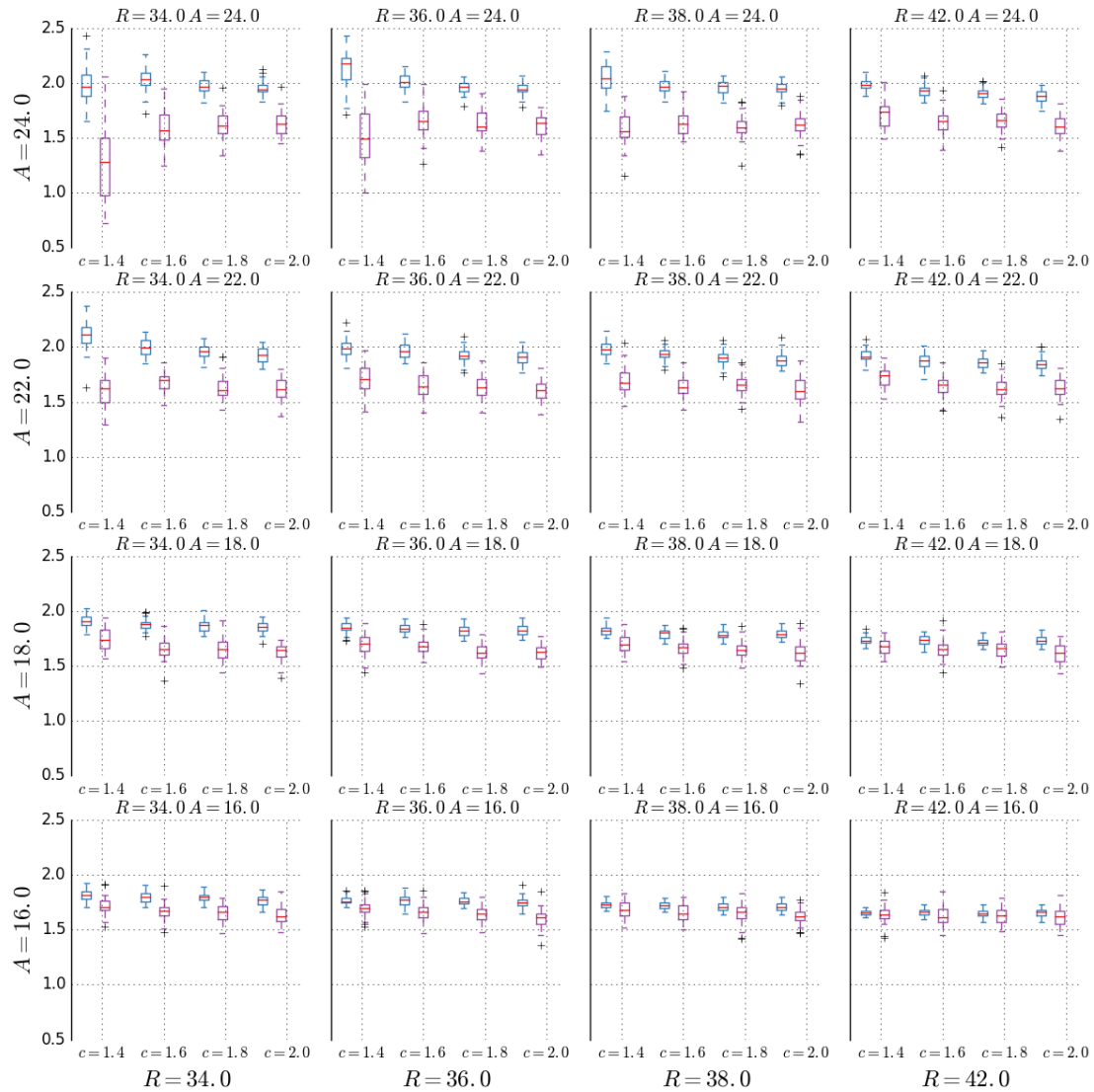


**Figure 44.** The flowrate distributions of two behaviours in the T-intersection corridor

The blue colour presents the flowrate distributions of grouping behaviour while the red colour presents the distribution of simulations of non-grouping behaviour. In this figure, each row represents a certain value of parameter  $A$  while each column stands for a value of parameter  $R$ .

In general, the flowrate of grouping behaviour was higher than the flow rate of non-grouping behaviour. Figure 45 summarizes the flowrate percentage difference between two behaviours. The difference varied in the range from 2% to 36 %.

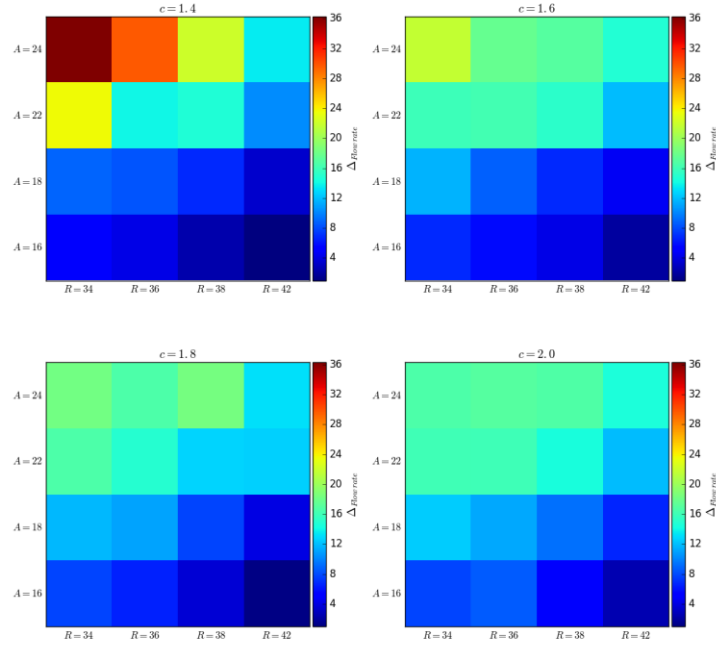


**Figure 45.** The heat map of the flowrate percentage difference in the T-intersection

At each value of parameter  $c$ , increasing attractive magnitude  $A$  makes  $\Delta_{flowrate}$  increase while the increase of repulsive strength  $R$  makes  $\Delta_{flowrate}$  descend. Figure 46 presents the turning angles of a testing distribution. The distribution was obtained when two crowds were moving in the intersection area.

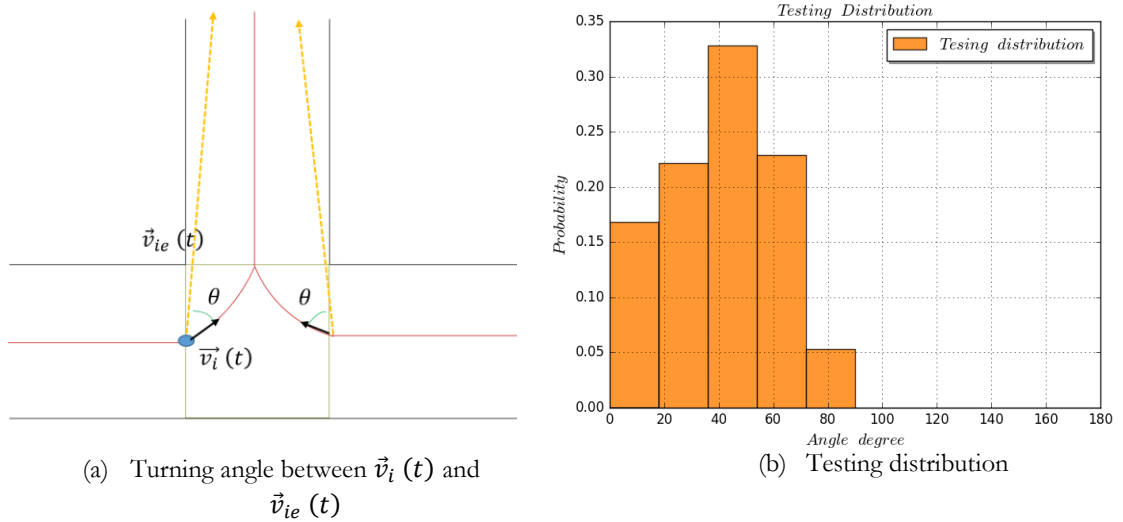


**Figure 46.** The testing distribution in the T-intersection corridor

The KL distances between the turning angle distributions of each behaviour and the testing distribution were analysed to investigate the movement of individuals in the corridor. Figures 47-50 presents the heat map of the KL distances of each behaviour at different parameter combinations.



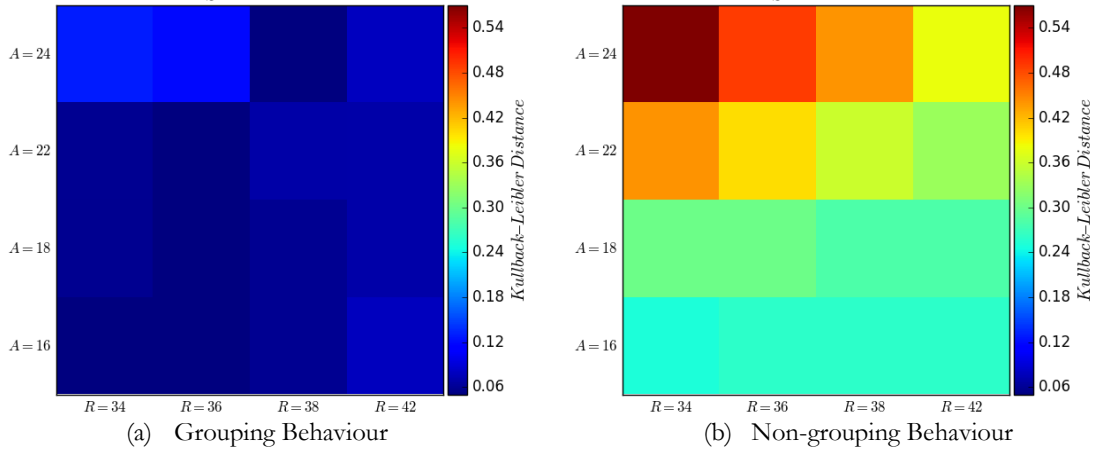


**Figure 47.** The heat map showing the KL distances in the T-intersection corridor with setting  $c=1.4$

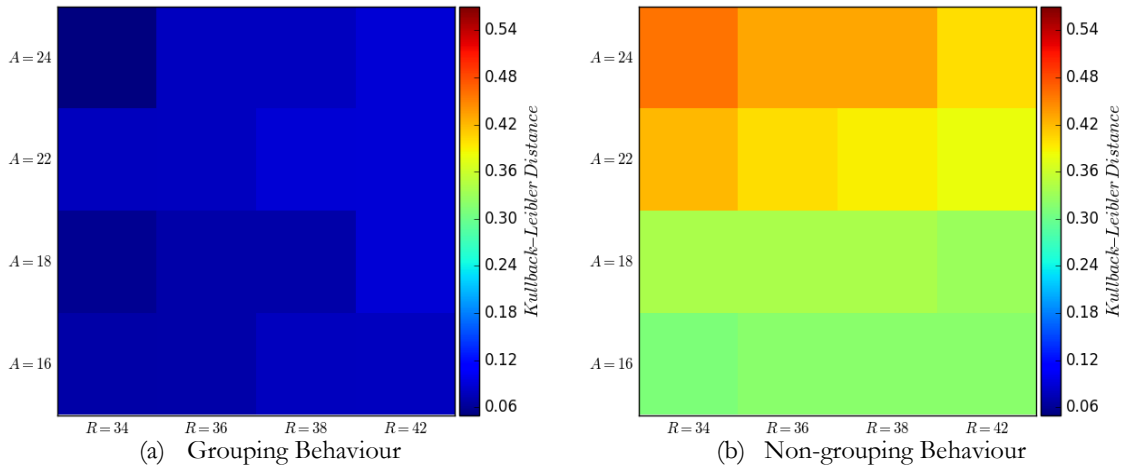


**Figure 48.** The heat map showing the KL distances in the T-intersection corridor with setting  $c=1.6$

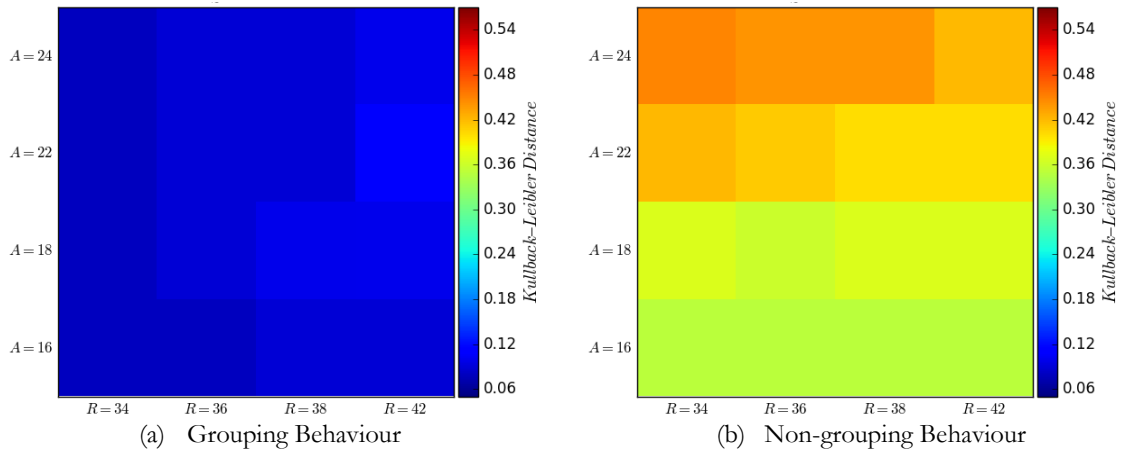


**Figure 49.** The heat map showing the KL distances in the T-intersection corridor with setting  $c=1.8$

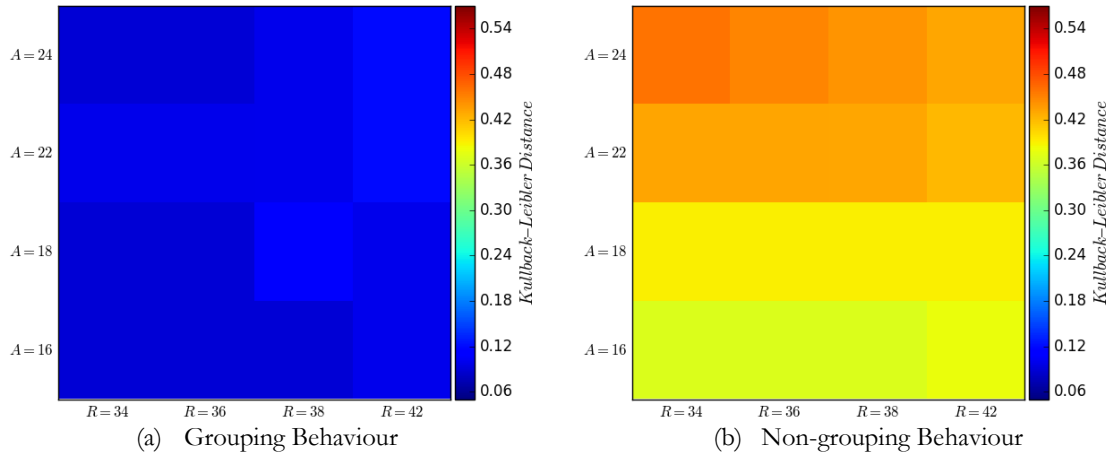


**Figure 50.** The heat map showing the KL distances in the T-intersection corridor with setting  $c=2.0$

In general, Figure 47-50 show the difference in the movement caused by grouping behaviour and non-grouping behaviour. The KL distances of grouping behaviour was very low across all parameter combinations. In contrast, the KL distances of non-grouping behaviour varied more greatly.

To investigate how individuals switched their attractors in the corridor, the networks of the strongest attractors of each individual over time were constructed.

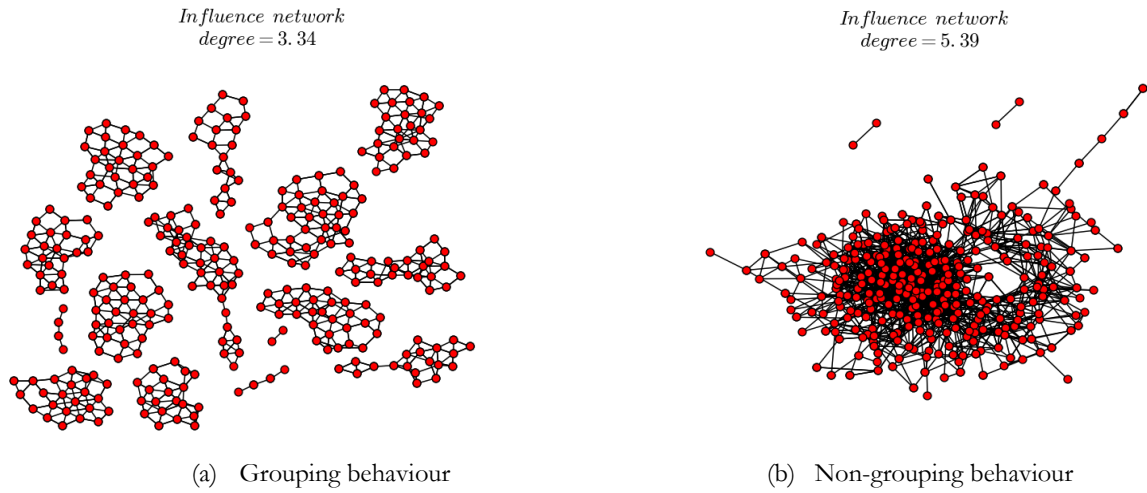


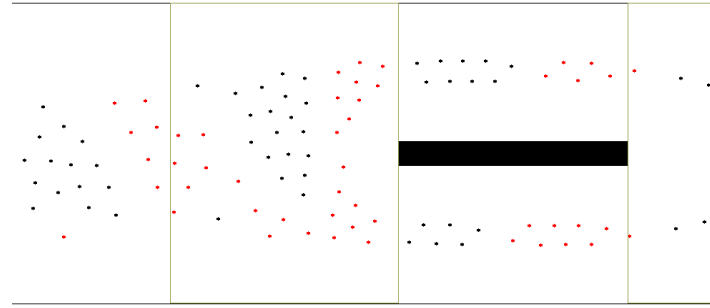
**Figure 51.** The influence networks of two behaviours in the T-intersection corridor with setting

$A=20.0$ ,  $R=36.0$ , and  $c = 1.4$ .

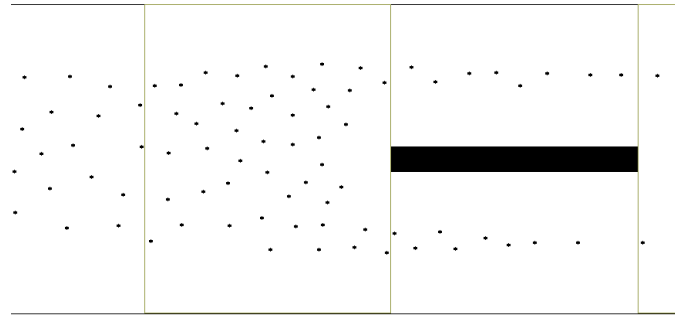
Figure 51 shows the networks of the two behaviours. In the network of grouping behaviour, clusters were formed. This result showed that individuals were in clusters during crowd movement. An individual switched on average 3.34 attractors. In contrast, the degree in the network of non-grouping behaviour was higher at 5.39. Clusters were not observed in this network. This result showed that the movement of non-grouping behaviour created turbulence.

### 6.3.4. The Difference in Corridor with an Obstacle

This section presents the comparison results between grouping and non-grouping behaviours in a corridor with an obstacle. Figure 52 shows the observation of two behaviours with setting  $A = 20$ ,  $R = 40$ , and  $c = 1.4$ .



(a) The movement of grouping behaviour



(b) The movement of non-grouping behaviour

**Figure 52.** The observation of grouping and non-grouping behaviours in the corridor with an obstacle

Simulation videos of these behaviours in a corridor with an obstacle can be viewed at [https://sites.google.com/site/vietquangvo/home#obstacle\\_corridor](https://sites.google.com/site/vietquangvo/home#obstacle_corridor)

Figure 52.a shows the emergence of clusters of individuals in the same group. In contrast, Figure 52.b does not show the emergence of clusters. Figure 53 presents the flow rate distributions of two behaviours at the 64 combinations of parameters ( $A$ ,  $R$ ,  $c$ ).

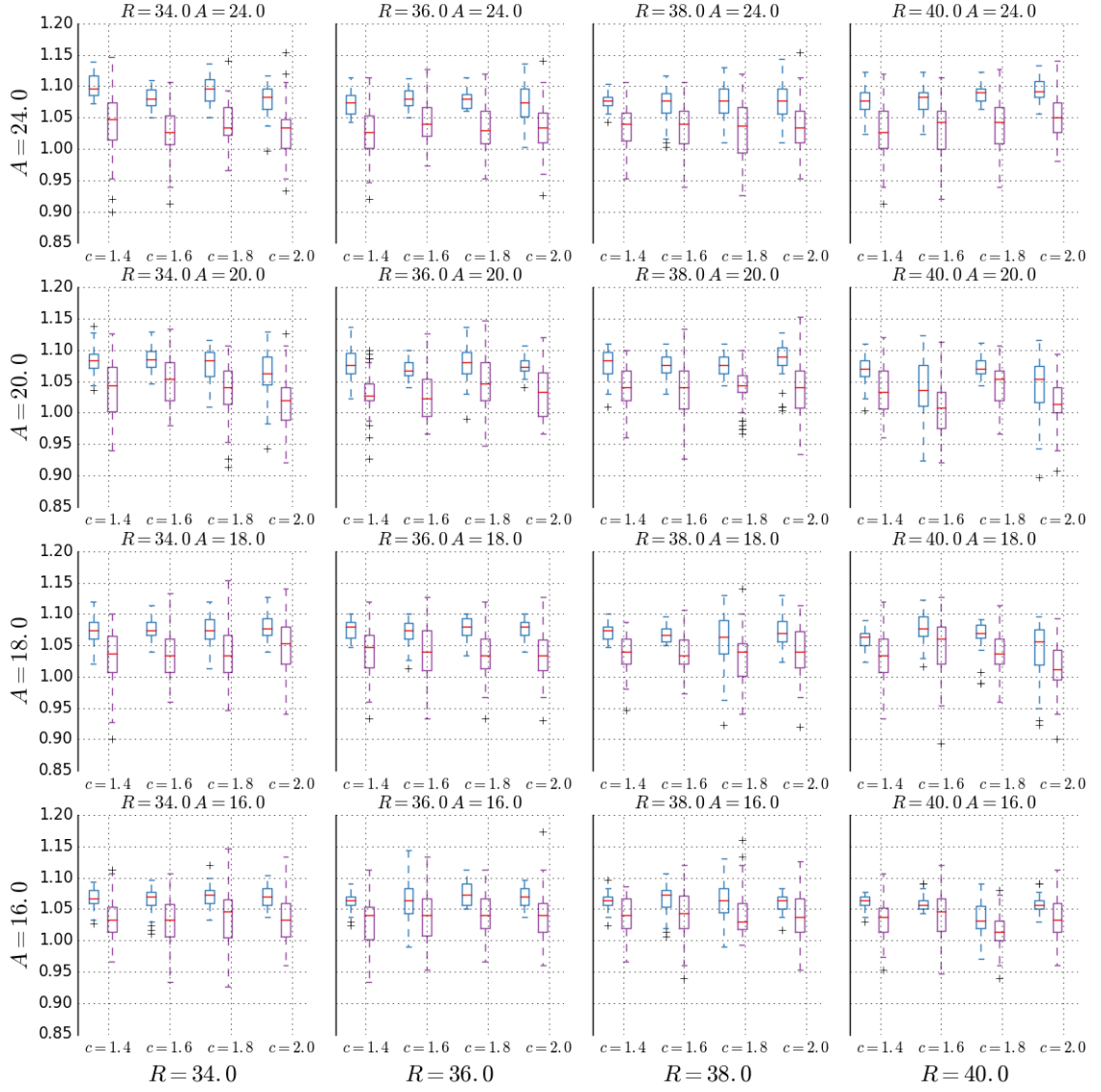


**Figure 53.** The flowrate distributions of grouping and non-grouping behaviours in the corridor with obstacle

The blue colour presents the flowrate distributions of simulations of grouping behaviour while the red colour presents the flowrate distributions of simulations of non-grouping behaviour. Each row represents a certain value of parameter  $A$  while each column stands for a value of parameter  $R$ .

Overall, the flowrates of grouping behaviour were higher than the flow rates of non-grouping behaviour. Figure 54 presents the heat map of the flowrate percentage difference between two behaviours. The difference varied in the range from 2.0% to 5.5 %.

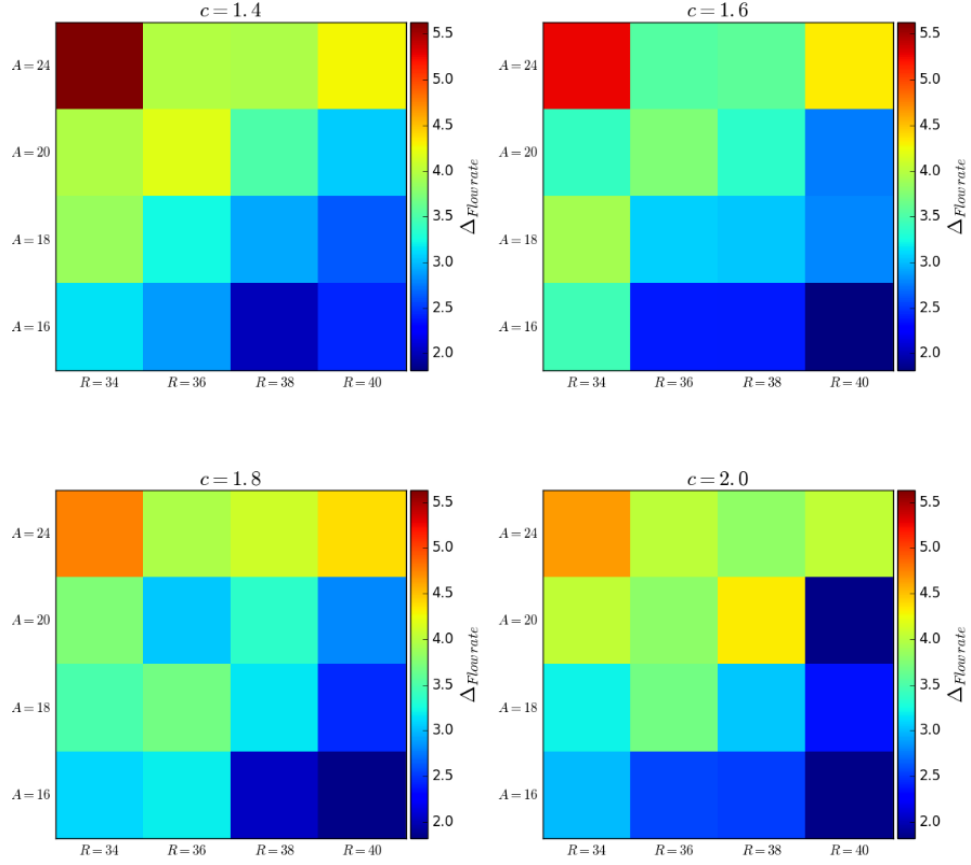
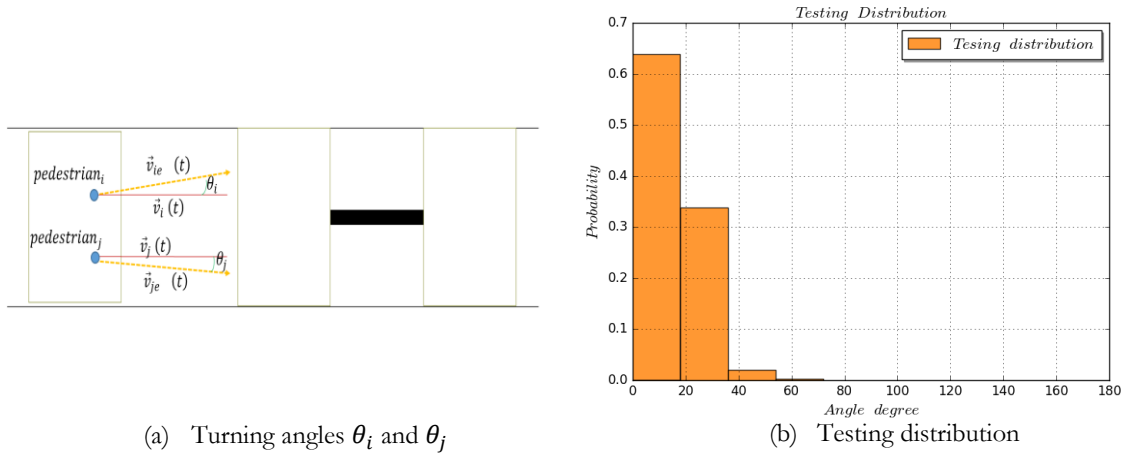


**Figure 54.** The heat map of the flowrate percentage difference in the corridor with an obstacle

At each value of parameter  $c$ , increasing attractive magnitude  $A$  makes  $\Delta_{flowrate}$  increase while the increase of repulsive strength  $R$  makes  $\Delta_{flowrate}$  descend. In this floor plan, a testing distribution was extracted from the movement of a small crowd in the corridor. The angles  $\theta$  between velocity vector and target vector of individuals were obtained when they were moving in the corridor. Figure 55 presents the turning angles and the testing distribution.



(a) Turning angles  $\theta_i$  and  $\theta_j$

(b) Testing distribution

**Figure 55.** The testing distribution in the corridor with an obstacle

Figures 56-59 present the heat map of the KL distances of each behaviour at different parameter combinations.

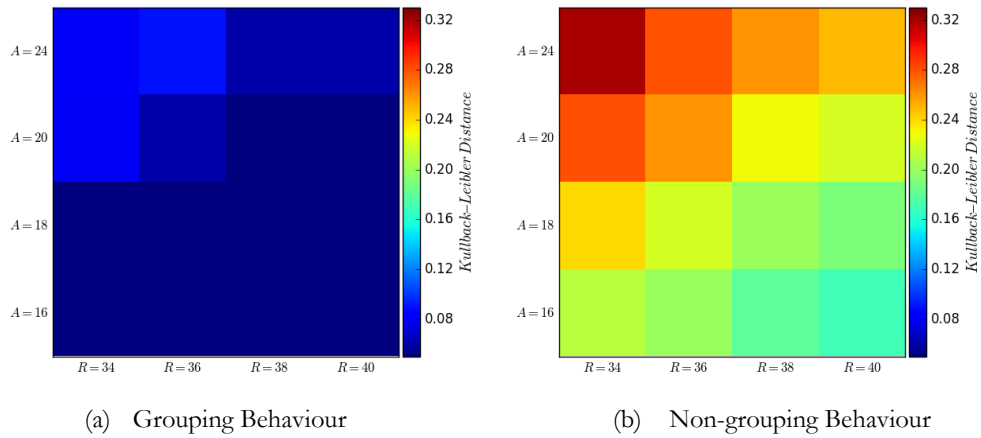


**Figure 56.** The heat map of the KL distances in the corridor with obstacle with setting  $c=1.4$

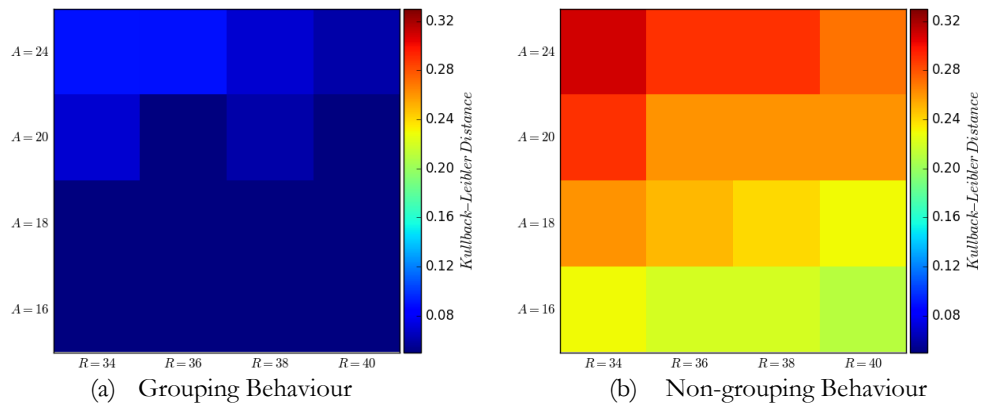


**Figure 57.** The heat map of the KL distances in the corridor with obstacle with setting  $c=1.6$

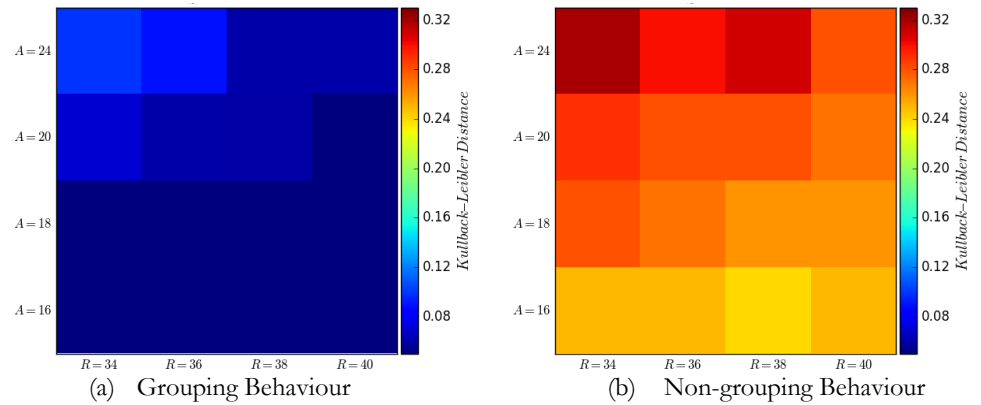


**Figure 58.** The heat map of the KL distances in the corridor with obstacle with setting  $c=1.8$

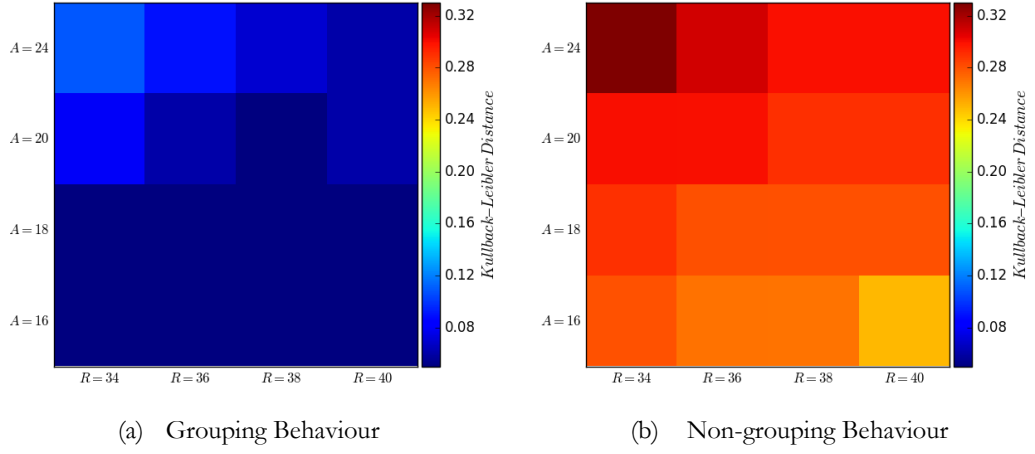


**Figure 59.** The heat map of the KL distances in the corridor with obstacle with setting  $c=2.0$

Overall, turning angle distributions of grouping behaviour were different from the turning angle distributions of non-grouping behaviours. In the KL distances of non-grouping behaviour, the increase of attractive magnitude  $A$  created higher KL distances. This result showed that higher attractive magnitude  $A$  made individuals moved more differently.

The influence networks of each behaviour were constructed to investigate how individuals behaved in the corridor, the networks of grouping and non-grouping behaviours were constructed.

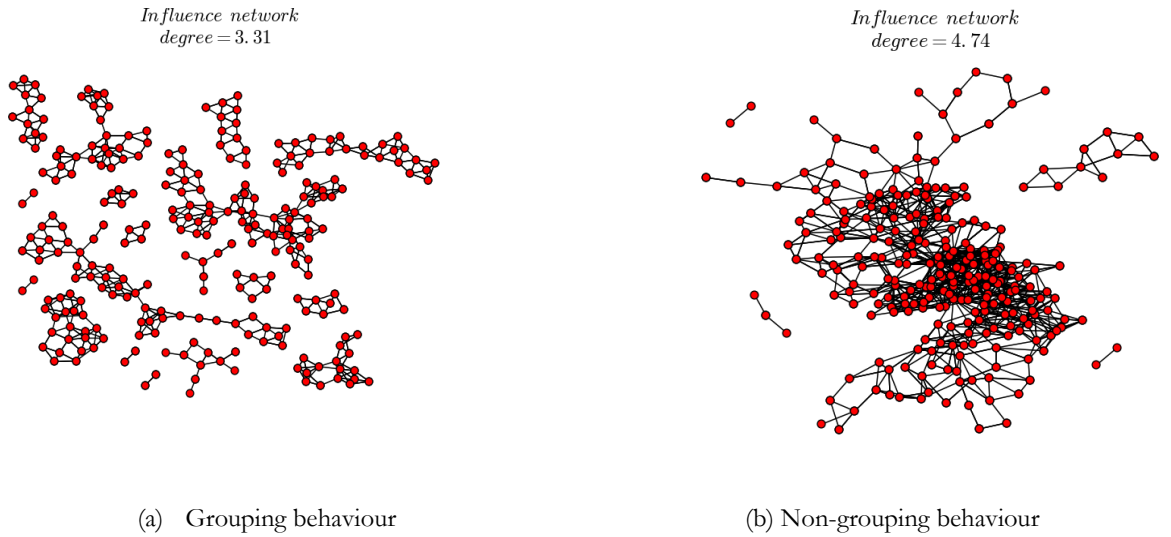


**Figure 60.** The influence networks of two scenarios in the corridor with an obstacle

with setting  $A=18.0$ ,  $R=40.0$ ,  $c = 1.4$ .

In the network of grouping behaviour, clusters were formed. This result confirmed that individuals were in clusters when they were moving in the corridor. An individual switched on average 3.31 attractors. In contrast, the degree in the network of non-grouping behaviour was higher at 4.74. Clusters were not observed in this network. This result showed that movement of non-grouping behaviour was turbulent.

## 6.4. Analysis of the Difference between Grouping and Non-grouping Behaviours

In general, the results from the simulations of grouping and non-grouping behaviours show that group behaviour facilitates effective crowd movement. The flowrates of grouping behaviours are consistently higher than the flowrates of non-grouping behaviours for the four typical floor plans. Grouping behaviour allows individuals to stay together with in-group members and to avoid other out-of-group members. Clusters form from grouping behaviours. These clusters move in an orderly fashion to exit corridors.

When clusters emerge in crowd movement, every individual receives the same amount of in-group and out-of-group forces. For instance, Figure 61 shows the forces acting on a tracked individual at different time steps  $t$  of a simulation of grouping behaviour.

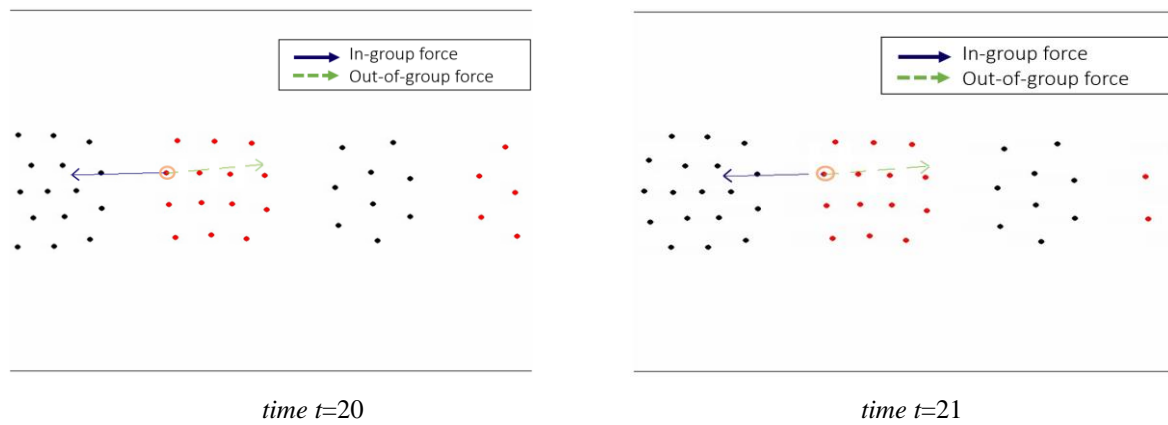


**Figure 61.** In-group and out-of-group forces acting on a tracked individual caused by grouping behaviour

The snapshots were captured in one simulation with setting  $A=2.0$ ,  $R=40$ , and  $c=1.4$ . The tracked individual is highlighted. The solid arrow shows in-group force acting on the tracked individual whereas dashed arrow presents out-of-group force. The length of each arrow is correlated with the magnitude of its corresponding force.

The forces acting on a tracked individual can be viewed at [https://sites.google.com/site/vietquangvo/home#force\\_balance](https://sites.google.com/site/vietquangvo/home#force_balance)

The emergence of clusters helps to maintain the balance between in-group and out-of-group forces acting on every individual over time. It allows individuals to stay together with their in-group members while they are exiting the narrowing corridor. Thus, individuals rarely change their attractors. This ordered movement of clusters prevents turbulence. The movement is significantly different from the movement caused by non-grouping behaviour. Non-grouping behaviour destroys the balance of in-group and out-of-group forces acting on each individual. Figure 62



shows an example of the rapid change in the direction and the magnitude of in-group and out-of-group forces caused by non-grouping behaviour.

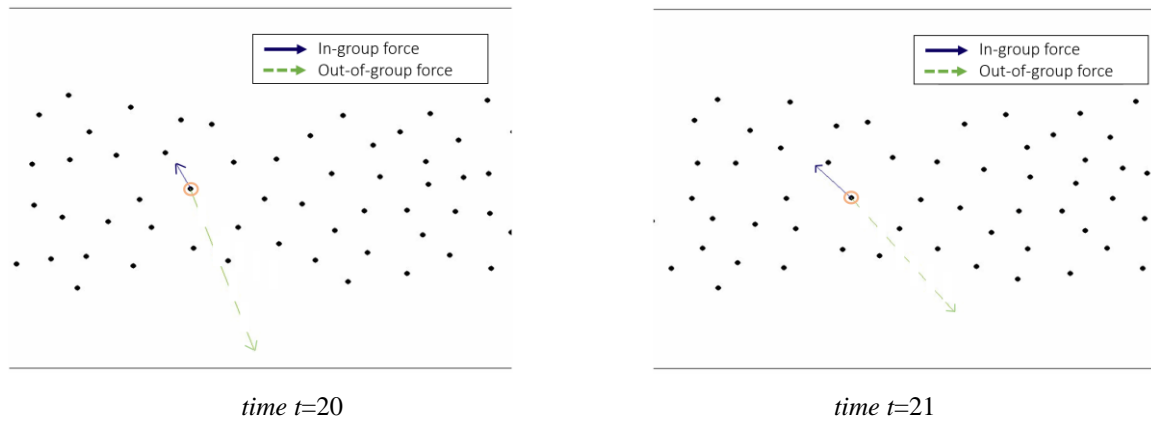


**Figure 62.** In-group and out-of-group forces acting on a tracked individual caused by non-grouping behaviour

The forces acting on a tracked individual can be viewed at  
[https://sites.google.com/site/vietquangvo/home#force\\_unbalance](https://sites.google.com/site/vietquangvo/home#force_unbalance)

Non-grouping behaviour makes individuals move irrationally. These individuals receive the unequal amount of in-group and out-of-group forces over time. As a result, they frequently switch attractors. Their turning angles vary greatly over time. Consequently, this movement creates turbulence and reduces flow rate. The flowrate percentage difference between grouping and non-grouping behaviour is significantly different. Especially, the flow rate difference is up to 36% in the T-intersection corridor followed by another value of 20% in the narrowing corridor. This difference emphasizes the effectiveness of the formation of clusters when crowds contain a large number of individuals.

## 7 Conclusion and Future Work

This chapter summarizes the findings of this study, and proposes recommendations for future work.

### 7.1. Conclusion

This study built a force-based model which is applicable to capture the grouping behaviour of individuals in an inhomogeneous crowd. The model is reasonable because it is extended from the base model that has been well accepted and validated. While the base model formulates the grouping behaviour of members in the same group, the extension takes into account the repulsive interaction between members of different groups in such inhomogeneous crowd.

While previous studies have focused on designing architectural layouts to prevent turbulence and to enhance flowrates for saving human lives in emergency situations, this study attempts to explore another solution to serve the purposes. By examining the impact of group interactions on crowd dynamics in the four typical layouts in evacuation simulation scenarios, this study finds that grouping behaviour helps to prevent turbulence to facilitate effective movement. Among the four widely used floor plans, T-intersection corridors have the largest flow rate difference between grouping and non-grouping behaviour. For crowds at public events, letting people stay together with their groups may be effective for crowd management when a large number of participants are egressing the venue.

### 7.2. Future Work

The need for modelling real-world crowds always motivates researchers to explore new aspects that can fully explain human crowd dynamics for floor plan optimization and crowd movement planning. This thesis have built a theoretical model, and empirical studies are needed to validate and modify it.

Previous studies have not collected data for real-world crowds that contain more than one group in order to calibrate the interactions of in-group members, and the interaction between in-group and out-of-group members. Thus, data acquisition is necessary to explore these interactions. Moreover, data collection also helps to explore whether the interaction between groups is different from real-world crowds at various places such as sport-like venues, work places, shopping malls, train stations, or schools. With the synthesis from different research fields and scientists, crowd behaviours are hopefully to be predictable in the near future.

# References

- Amigo, E., Gonzalo, J., Artiles, J., and Verdejo, F., (2009). A comparison of extrinsic clustering evaluation metrics based on formal constraints. *Information Retrieval*. vol.12, page 461.
- Almeida, E. J., Rosseti, R., and Coelho, A. L., (2011). Crowd Simulation Modeling Applied to Emergency and Evacuation Simulations using Multi-Agent Systems. In *DSIE'11 - 6th Doctoral Symposium on Informatics Engineering*, 6th Doctoral Symposium on Informatics Engineering, Porto, pages 93–104.
- Aveni, A., (1977). The not-so-lonely crowd: friendship groups in collective behaviour. *Sociometry* vol.40, pages 96–99.
- Bhattacharya, K., Vicsek, T., (2010). Collective decision making in cohesive flocks. *New Journal of Physics*, vol. 12.
- Bertin, E., Gregoire, G., 2009. Hydrodynamic equations for self-propelled particles: microscopic derivation and stability analysis: *Journal of Physics A: Mathematical and Theoretical*, vol. 42.
- Bonabeau, E., (2002). Agent-based modelling: Methods and Techniques for Simulating Human Systems. *PNAS*, vol. 99, pages 7280–7287.
- Burstedde, C., Klauck, K., Schadschneider, A., and Zittartz, J. (2001). Simulation of pedestrian dynamics using a two-dimensional cellular automaton. *Physica A: Statistical Mechanics and its Applications*, vol. 295(3), pages 507-525.
- Challenger, R., Clegg, C. W., Robinson, M. A. (2010). Understanding Crowd Behaviours, Vol.2: Supporting theory and evidence (London, The Stationery Office (TSO)), Cabinet Office, ISBN 10: 0114302049.
- Cocking, C. and Drury, J. (2008). The mass psychology of disasters and emergency evacuations: A research report and implications for the Fire and Rescue Service. *Fire Safety, Technology and Management*, vol.10, pages 13-19.
- Cocking, C., Drury, J. and Reicher, S. (2009). The psychology of crowd behaviour in emergency evacuations: Results from two interview studies and implications for the Fire & Rescue Services. *Irish Journal of Psychology. Special Edition: Psychology and the Fire & Rescue Services*, vol. 30(1-2), pages 59-73.
- CNN, <http://edition.cnn.com/2013/04/17/us/gallery/boston-marathon-eyewitness/>
- Daniel, S., (2012). The Nature of Code: Simulating Natural Systems with Processing. ISBN-10: 0985930802.
- Davies, P., (2013). A mathematical model of the London riots and their policing. *Nature Scientific Reports*, vol.3, pages 1303.

- Dougall, A.L., Hyman, K.B., Hayward, M.C., McFeeley, S. & Baum, A. (2001). Optimism and traumatic stress: The importance of social support and coping. *Journal of Applied Social Psychology*, vol.31, pages 223-245.
- Drury, J. and Winter, G. (2004). Social identity as a source of strength in mass emergencies and other crowd events. *International Journal of Mental Health* (special issue on “Coping with disasters: The mental health component”), vol.32, pages 77-93.
- Drury, J., Cocking, C., and Reicher, S. (2009). Everyone for Themselves? A Comparative Study of Crowd Solidarity Among Emergency Survivors. *British Journal of Social Psychology*, vol. 48, pages 487– 506.
- Drury, J., Cocking, C., and Reicher, S. (2009). The nature of collective resilience: Survivor reactions to the 2005 London bombings. *International Journal of Mass Emergencies and Disasters*, vol. 27, pages 66–95.
- Dugan, L., and Daren, F., (2015). Strategic Responses to the Boston Marathon Bombing. *Oxford Research Reviews*.
- Ester, M., Kriegel, P. H., Sander, J., Xu, X., (1996). A density-based algorithm for discovering clusters in large spatial databases with noise. In *Proceedings of ACM SIGKDD Conference*.
- Fehlberg, E., (1969). Low-order classical Runge-Kutta formulas with step size control and their application to some heat transfer problems. *NASA Technical Report*, vol. 315.
- Georgeff, M.P., Ingrand, F.F, (1989). Decision-Making in an Embedded Reasoning System. *International Joint Conference on Artificial Intelligence*, pages 972-978.
- Grosshandler, W., Bryner, N., Madrzykowski, D., Kuntz, K., (2005). Report of the Technical Investigation of the Station Nightclub Fire. *NIST NCSTAR 2*: vol. 1.
- Hafstein, S. F., Chrobok, R., Pottmeier, A., Schreckenberg, M., Mazur, F. C., (2004). A High Resolution Cellular Automate Traffic Simulation Model with Application in a Freeway Traffic Information System. *Comp-aided Civil Engineer*, vol. 19(15), pages 338-350.
- Hankin, B., & Wright, R. (1958). Passenger Flow in Subways. *OR*, vol. 9(2), pages 81-88.
- Haslam, S. A., O'Brien, A., Jetten, J., Vormedal, K., and Penna, S. (2005). Taking the strain: Social identity, social support and the experience of stress. *British Journal of Social Psychology*, vol. 44, pages 355-370.
- Hoogendoorn, S.P., Duive, .D.C., Daamen, W., (December 2013). State-of-the-art crowd motion simulation models. *Transportation research part C*, vol. 37, pages 193-209.
- Hoogendoorn, S.P., Bovy, P. H.L (2003) Simulation of pedestrian flows by optimal control and differential games. *Optimal Control Applications and Methods*, vol. 24, pages 153-172.
- Helbing, D., Molnar, P., (1995) Social Force Model for Pedestrian Dynamics. *Physical Review E*, vol. 51.

- Helbing, D., Farkas, I., Vicsek, T., (2000). Simulating Dynamical Features of Escape Panic. *Nature*, pages 4487-4490.
- Helbing, D., Farkás, I. J., Molnár, P., Vicsek, T., (2002). Simulation of pedestrian crowds in normal and evacuation situations. M. Schreckenberg, S. D. Sharma, (Eds.), *Pedestrian and Evacuation Dynamics*. Springer, Berlin, Germany, pages 21–58.
- Helbing, D., Buzna, L., Johansson, A., Werner, T., (2005). Self-organized Pedestrian Crowd Dynamics Experiments Simulation Design Solution. *Transportation Science*, vol. 39, pages 1-24.
- Helbing, D., Johansson, A., Al-Abideen, H., (2007). Dynamics of crowd disasters: An empirical study. *Physical Review E*, vol. 75(4).
- Helbing, D., Mukerji, P., (2012). Crowd disasters as systemic failures: analysis of the love parade disaster *EPJ Data Sci*, vol. 1(7).
- Hevner, R. A., March, S. T., Park, J., Ram, S., (2004). Design science in information systems research. *Mis Quarterly*, 28(1):75\_105, 2004. ISSN 0276-7783.
- Huepe, C., Aldana, M., (2008). New Tools for characterizing swarming systems: A comparison of nominal models. *Physical A*, vol. 387, pages 2809-2822.
- Janis, I. L. and Leventhal, H. (1968). Human reactions to stress. In E. F. Borgatta and W. W. Lambert (Eds.), *Handbook of Personality Theory and Research*, pages 1041–1085. Chicago: Rand-McNally.
- Johnson, R. L., (2008). Microcolony and Biofilm Formation as a Survival Strategy for Bacteria. *Journal of Theoretical Biology*, vol. 251, pages 24-34.
- Katz, Y., Tunstrom, K., Ioannou, C., Couzin, I., (2011). Inferring the structure and dynamics of interactions in schooling fish. *PNAS*, vol. 108, pages 18720-18725.
- Killian, L. M. (1972). *Collective Behavior*. Englewood Cliffs, NJ: Prentice-Hall.
- Liu, Y., Liu, D. M., Norman, B., (2011). Analysis of evacuation performance of merging points in stadiums based on crowd simulation. In *Proceedings of the 12th Conference of the International Building Performance Simulation Association*, pages. 2651–2658.
- Lukeman, R., Li, Y., Edelstein-Keshet, L., (2010). Inferring individual rules from collective behaviour. *PNAS*, vol.107 (28), pages 12576-12580.
- Macal, C. and North, M. (2011). Introductory Tutorial: Agent-based Modelling and Simulation. In *Proceedings of the 2011 Winter Simulation Conference*, pages 1456-1469.
- March, T. S., Smith, F. G., (1995). Design and natural science research on information technology. *Decision Support Systems*, 15(4):251 \_ 266, 1995. ISSN 0167-9236.
- Mogilner, A., Edelstein-Keshet, L., Bent, L. , Spiros, A., (2003). Mutual Interactions, Potentials, and Individual Distance in a Social Aggregation. *Journal of Mathematical Biology*, pages 353-389.

- Moussaid, M., Perozo, N., Garnier, S., Helbing, D., Theraulaz, G., (2010). The Walking Behaviour of Pedestrian Social Groups and Its Impact on Crowd Dynamics. *PLoS ONE*, vol. 5(4).
- Moussaid M, Helbing D, Theraulaz G., (2011). How Simple Rules Determine Pedestrian Behaviour and Crowd disasters. *Proceedings of National Academy Sciences, USA*, vol.108, pages 6884–6888.
- Myers, D. J., and Caniglia, S. B.,(2004). All the rioting that's fit to print: Selection effects in national newspaper coverage of civil disorders. *American Sociological Review*, vol. 69 (4), pages 519–543.
- Neumann, V. J., (1966).Theory of Self-Reproducing Automata, *University of Illinois Press*, Urbana.
- Orsogna, M. R., and Chuang, Y. L., Bertozzi, A. L., Chayes, L. S., (2006). Self-Propelled Particles with Soft-Core Interactions: Patterns, Stability, and Collapse. *Physical Review Letters*, vol. 96.
- Pelechano, N., Badler, N., (2006). Modelling Crowd and Trained Leader Behaviour during Building Evacuation. *IEEE Computer Graphics and Applications*, 26 (6), pages 80-86.
- Price, M. C., (2015), Boston Marathon Bombing and Experiences of Solidarity: The Race to Understanding. *Master of Science Thesis, Virginia Commonwealth*.
- Quarantelli, E. L., (1954). The nature and conditions of panic. *American Journal of Sociology*, vol. 60, pages 267-275.
- Quarantelli, E. L., (1957). The behavior of panic. *Sociology and Social Research*, vol. 60, pages 187–194.
- Reynolds, C. W., (1987). Flocks, Herds and Schools: A Distributed Behavioural Model. *SIGGRAPH*, Proceedings of the 14th annual conference on Computer graphics and interactive techniques, ACM, New York, NY, USA, pages 25–34.
- Reynolds, C. W., (1999). Steering behaviours for autonomous characters. In the *Proceedings of Game Developers Conference*, San Jose, California, pages 763-782.
- Reicher, S., Drury, J., (2011). Collective Identity, Political Participation and The Making of The Social Self. In A. Azzi, X. Chryssochoou, B.Klandermans, & B. Simon (Eds.), *Identity and participation in culturally diverse societies: A multidisciplinary perspective*.Oxford, England: Wiley-Blackwelli, pages 158–176.
- Ronchi, F., Nieto, U. F., Criel, X., Reilly, P. (2016). Modelling large-scale evacuation of music festival. *Fire Safety 2016*, vol. 5, pages 11-19.
- D.A. Schön. The reflective practitioner: how professionals think in action. Basic Books, 1983. ISBN 9780465068784. URL <http://books.google.com/books?id=ceJIWay4-jgC>.
- Shendarkar, (2008). Crowd simulation for emergency response using BDI agents based on immersive virtual reality. *Simulation Modelling Practice and Theory*, 16(9), pages 1415–1429.

- Stott, C., Adang, O., Livingstone, A., Schreiber, M., (2007). Variability in The Collective Behaviour of England fans at Euro2004: 'Hooliganism', public order policing and social change, *Eur. J. Social Psychol*, vol. 37, pages 75–100.
- Suma, Y., Yanagisawa, D., and Nishinari, K. (2011). Anticipation Effect in Pedestrian Dynamics: Modelling and Experiments. *Physica A: Statistical Mechanics and its Applications*, 391(1-2), pages 248-263.
- Sun, Q., (2014). A Configurable Agent-Based Crowd Model with Generic Behaviour Effect Representation Mechanism. *Journal of Computer-Aided Civil and Infrastructure Engineering*, vol. 29(7), pages 531-545.
- Torrens, P. M. and McDaniel, A. W., (2013).Modelling geographic behaviour in riotous crowds. *The Annals of the American Association of Geographers*. vol. 103.
- Vicsek, T., Czirok, A., Ben-Jacob, E., Cohen I, I., Shochet, O.,(1995). Novel type of phase transition in a system of self-driven particles. *Physical Review Letters*, vol. 75.
- Vizzari, G., Manenti, L., Crociani, L., (2013). Adaptive Pedestrian Behaviour for The Preservation of Group cohesion. *Complex Adaptive Systems Modelling*, pages 1-7.
- Vihás, C., Georgoudas, G. I., Sirakoulis, C. G., (2012). Follow-the-leader Cellular Automata based Model Directing Crowd Movement, *Lecture Notes in Computation. Science*, vol. 7495, pages 752–762.
- Viscido, V. S., Parrish, K. J., Grünbaum, D., (2005). The effect of population size and number of influential neighbours on the emergent properties of fish schools. *Ecological Modelling*, vol.183, pages 347-363.
- Weidmann, U., Uwe, K., Schreckenberg, M. (2012). Pedestrian and Evacuation Dynamics 2012. *Springer*.
- Winter, H., (2012). Modelling Crowd Dynamics during Evacuation Situations Using Simulation. *STOR601: Project, Lancaster University*.
- Wijermans, (2013). CROSS: Modelling Crowd Behaviour with Social-Cognitive Agents. *Journal of Artificial Societies and Social Simulation*, vol. 16(4).
- Wirz, M., Franke, T., Roggen, D., Mitleton-Kelly, E., Lukowicz, P. .,Troster, G., (2013). Probing crowd density through smartphones in city-scale mass gatherings. *EPJ Data Science*, vol. 2(1).